UNIVERSITY OF OKLAHOMA

GRADUATE COLLEGE

PERFORMANCE SEAL TESTING THROUGH THE EVALUATION OF THE LEAK RATE OF THE MECHANICAL SEAL

A THESIS

SUBMITTED TO THE GRADUATE FACULTY

in partial fulfillment of the requirements for the

Degree of

MASTER OF SCIENCE

By

MOUSSA COULIBALY

Norman, Oklahoma

2024

Downloaded from SHAREOK. Persistent Handle URL: https://hdl.handle.net/11244/340346

PERFORMANCE SEAL TESTING THROUGH THE EVALUATION OF THE LEAK RATE OF THE MECHANICAL SEAL

A THESIS APPROVED FOR THE
SCHOOL OF AEROSPACE AND MECHANICAL ENGINEERING

BY THE COMMITTEE CONSISTING OF

Dr. Zahed Siddique, Chair

Dr. Yingtao Liu

Dr. Shivakumar Raman

© Copyright by MOUSSA COULIBALY 2024
All Rights Reserved.

ACKNOWLEDGMENTS

I would like to express my deepest and most sincere gratitude to my research advisor and mentor, Dr. Zahed Siddique, for investing his time, finances, and energy during my tenure as a graduate student. Since my admission, Dr. Siddique has been my greatest support at the university. He has believed in me and supported me in ways that still amaze me. Dr. Siddique, thank you infinitely for your love and endless support. I would not have been able to pursue my master's degree without the research opportunity you provided. From our very first meeting, your personality was infectious. You gave me a chance when I had no other, allowed me to work on the projects I wanted, and guided me through the daily steps of those projects, permitting me to make mistakes and grow as a researcher. I hope I have made you proud, Dr. Siddique. I do not know what kind of leader I will become tomorrow, but if I could be half as great as you are, I would consider myself a very successful mentor. From the bottom of my heart, THANK YOU! I shall forever be in your debt.

Besides my advisor, I would like to thank my committee members, Dr. Yingtao Liu and Dr. Shivakumar, for their tremendous support and guidance. I had the honor of taking a class with Dr. Liu, and I am sincerely grateful for all the knowledge you bestowed upon me, whether on additive manufacturing, the research process, or life in general. Dr. Raman is an amazing person, and it is an honor to have you on my committee.

My sincere thanks to all the AME faculty and staff. I am particularly grateful to Dr. Ramkumar Parthasarathy, Samarpita Gosh, Bethany Burkland, and AME Machinists Billy Mays and Greg Williams.

I would like to personally thank all my fellow student researchers under Dr. Siddique for their contributions and continuous support on this project. Thank you to Adam Bicak, Jonas Manchester, Monjur Bhuiyan, Ahmed Sakib, Philip Resnick, and Alfredo Corral. You mentored and guided me so much these past few years on this project, and I would be remiss if I did not include everyone's name in this section. Special gratitude to my lab partners Nicholas Khor and Cooper Whitnah. You have worked with me day and night on this project. This thesis would not have seen the light without you. I hope you are as proud of this work as I am thankful for working with you and learning from you.

I would like to thank my family, parents, siblings, nieces, nephews, and all my loved ones for their unwavering love, support, and prayers. This work is also yours. I could not have done it without you. You are my source of strength and guidance.

Last but certainly not least, I would like to express my deepest gratitude to الله subhana wa ta'ala for everything, simply everything. Ya Allah, I owe you everything.

Table of Contents

ACKNOWLEDGMENTS iv

Table of Contents vi

List of Figures ix

Abstract xi

Chapter 1: Introduction 1

1.1 Research Motivation 1

1.2 Research Scope 2

1.3 Research Objectives 2

1.4 Thesis Outline and Scope of Study 3

Chapter 2: Literature Review 4

2.1 Introduction 4

2.2 Background 4

2.3 Rotary Seal 7

2.4 Mechanical Seal 8

Chapter 3: Experimental Steup 12

3.1 Introduction 12

3.2 Modules with same parameters 14

3.2.1 MTS and LVDT sensors 14

3.2.3 DUT 16

3.3 Modules with different parameters 18

3.3.1 Motor 18

3.4 Other Components of the Systems 19

3.4.5 Argon and Compressed Air Gases 19

3.4.1 Control Panel and P.I.D controller 20

3.4.2 Cooling system 22

3.4.3 Test Stand 24

3.4.4 Vacuum Pump 25

3.4.6 Complete Mechanical Test System 27

3.4 Assembly 28

3.6 Data Acquisition and Processing 32

3.6.1 User Interface (LABVIEW) 32

3.6.2 Matlab 33

Chapter 4: Leak Rate Analysis 34

4.1 Leak rate calculation and testing conditions 34

4.2 Leak rate of individual seals 36

4.3 Testing seal beyond RPM range 38

4.4 Failures Analysis 44

4.4.1 Seal failure 45

4.4.2 System malfunction failure 46

Chapter 5: Conclusion and Future Work 49

5.1 Conclusion..... 49

5.2 Future Work 52

References.....53

Appendix A: Nomenclature and Acronyms.....55

List of Figures

Figure 1: Cross-section of an elastomeric lip on a rotary shaft [10] 8

Figure 2: Mechanical seal nomenclature [11] 10

Figure 3: Fluid schematic of the 10K- RPM rig [13] 13

Figure 4: MTS sensor schematic 15

Figure 5: Schematic of the components of the MTS sensor [12] 16

Figure 6: Simplified schematic of the DUT 17

Figure 7: Detailed DUT nomenclature 18

Figure 8: Motor on the horizontal position 19

Figure 9: Compressed air supply 20

Figure 10: Control panel for 10K system [13] 21

Figure 11: Schematic of cooling blocks 23

Figure 12: Copper cooling wire loop 24

Figure 13: Test stand [12] 25

Figure 14: Vacuum pump 26

Figure 15: Vacuum pump schematic on DUT 26

Figure 16: Complete mechanical schematic of the test system [14] 27

Figure 17: Workbench and primary DUT chamber 28

Figure 18: Fully mounted DUT 29

Figure 19: Fully mounted DUT attached to the motor 29

Figure 20: Testing system on the vertical position 31

Figure 21: LABVIEW user interface 32

Figure 22: Volume leak rate of a seal showing stabilization period with estimated start and end points 35
Figure 23: 75 hours leak rate at 10,000 RPM 37
Figure 24: 25 hours leak rate at 10,000 RPM 38
Figure 25: 50 hours leak rate at 6500 RPM 39
Figure 26: 70 hours leak rate at 7500 RPM 40
Figure 27: 48 hours leak rate at 8500 RPM 41
Figure 28: 24 hours leak rate at 9000 RPM 42
Figure 29: 48 hours leak rate at 9000 RPM 43
Figure 30: 96 hours leak rate at 9000 RPM 44
Figure 31: 120 hours leak rate at 9000 RPM 45
Figure 32: Shattered spring collar 47
Figure 33: Leak rate behavior of test experiencing shattered collar 48

Abstract

Sealing technology is important across various industries, particularly within the oil and gas sector. This technology encompasses the capability to obstruct the unrestricted flow of undesirable substances into reservoirs. Its significance lies in prolonging the lifespan of rotating dynamic systems like bearings in compressors or pumps. In the oil and gas industry sector, where rotating equipment is crucial for numerous drilling and production operations, maintaining the functionality of such equipment is imperative. Given the potentially hazardous nature of many fluids in oil and gas sector, consistent restriction of containments of these substances in dynamic applications is vital not only for equipment longevity but also for the safety of operators. While polymers are commonly used in dynamic applications due to their cost-effectiveness, their utility can be constrained by harsh environmental conditions such as surface speed or temperature. Consequently, this limitation has spurred a demand for the advancement of mechanical seals to address the shortcomings of polymer usage in dynamic settings.

This thesis focuses on assessing the leak rate of mechanical seals. Experimental tests are structured into two main sections. The first section examines the leak rate performance of a mechanical seal tested under the manufacturer's specified conditions at ten thousand (10,000) RPM. The second section investigates the performance of a seal subjected to operating conditions beyond those recommended by the manufacturer.

Through the analysis of these results, a comprehensive understanding of how leak rate efficiency varies with time and rotational speed emerges. Furthermore, the research sheds light on the leak rate patterns exhibited by a mechanical seal nearing failure. This investigation serves as a testament to the ongoing necessity and significance of experimental evaluation in appraising

mechanical sealing technology, despite the advancements in modern engineering simulation software.

Chapter 1: Introduction

1.1 Research Motivation

The scope of sealing technology is vast and fundamental across many industries. Use of seals plays a crucial role in mechanical design by effectively controlling the passage of gas, fluids, or solids across boundaries. Some of the common sealing technology include static, rotary, and reciprocating seals, with the widely known O-ring being a common example. Nonetheless, O-rings, like other seals, have limitations influenced by environmental conditions. These conditions include but are not limited to the temperature of the substance or equipment, the linear and rotational speed of the seal, and the pressure the device is subject to.

The oil and gas sector is one industry where sealing technology holds immense importance. Rotating equipment like pumps and compressors, integral to numerous processes in this industry, must effectively seal media that can be hazardous and volatile under varying conditions. Ensuring the performance of seals in such equipment is critical to prevent contaminants from compromising essential components, thus safeguarding both equipment longevity and operator safety.

Given the diverse and demanding operational environments of rotating equipment, there is a pressing need for the development of new seal materials and design. However, the wide range of conditions makes establishing standardized performance data challenging, hindering informed decision-making within the industry. This thesis aims to address this challenge by proposing a methodology to evaluate performance data on seals under extreme operational conditions, employing a platform-based testing approach for rotating seal design setups.

1.2 Research Scope

The performance of mechanical seals is influenced by the unique operational conditions of the machinery they are installed in. These conditions, including rotary speed, temperature, and pressure, directly impact the seal's effectiveness.

There is a plethora of ways of evaluating seal performance, but this thesis focuses on evaluating seal performance primarily through the examination of leak rates. With the aforementioned perspective, three hypotheses have been developed for this research:

1. The duration of mechanical seal usage affects leak rate efficiency
2. Rotary speed directly correlates with leak rate of the mechanical seal
3. Harsh operating conditions, such as high rotary speeds, may precipitate premature mechanical seal failure

1.3 Research Objectives

In examining mechanical seal performance via leak rate analysis, numerous experiments were conducted under consistent testing conditions to maintain research uniformity. The aim is to assess and derive conclusions regarding mechanical seal leak rates. The primary objectives of this research are outlined below:

1. Explore the impact of mechanical seal usage on leak rate efficiency.
2. Investigate the relationship between rotary speed and mechanical seal leak rates.
3. Subject mechanical seals to non-standardized conditions to induce seal failure.
4. Analyze the leak rate behavior of mechanical seal experiencing failure

1.4 Thesis Outline and Scope of Study

The scope of this research focuses on conducting experimental investigation on leaking rate of mechanical seal. The experiment is conducted by attaching the mechanical seal to a rotating machinery and is performed under consistent conditions. To better conduct this research, a concise and well-developed outline was followed. The research outline used is classified below.

1. Literature Review (Chapter 2): Literature review on rotary seals, mechanical seals and rotary machinery. The review process includes analysis of journal articles, books, and other related technical publications.
2. Methodology (Chapter 3): This chapter provides a detailed explanation of the laboratory equipment, testing system and component schematics utilized in the experiments. The chapter also details the assembly process of the main rotary machinery used as well as the data acquisition system and processing into visual figures to be analyzed.
3. Results and analysis (Chapter 4): After performing multiple tests to evaluate the research objectives mentioned above, the data were analyzed to validate the research hypothesis. An extensive analysis of the processed data helped in evaluating the leak rate of the mechanical seal and ultimately develop a deeper understanding of the mechanical seal performance and behavior.

Chapter 2: Literature Review

2.1 Introduction

This section provides a comprehensive examination of the significance, necessity, applications, and various types of seals. It also delves into a thorough review and synthesis of prior research concerning related areas, including prognostics of mechanical seals. By consolidating insights from previous studies, this section aims to establish a robust foundation for understanding the context and relevance of the current research within the broader field of seal technology.

2.2 Background

In the oil and gas industry, ensuring the reliability and prolonged lifespan of rotary and reciprocating equipment, including compressors, pumps, turbines, and engines, is crucial to meet and preserve the efficiency demands of oil field operations.

A seal is often presented in a circular shaped object or torus, commonly used to contain fluids within a designated space while preventing the infiltration of dirt, dust, mud, water, or any other undesirable substances. These seals operate by exerting pressure against a counterpart surface to close the gap between two interacting components. Seals are typically crafted from materials with high levels of flexibility and elasticity like elastomers, allowing them to adapt to the surfaces they encounter. They can also be manufactured using other polymers such as Polytetrafluoroethylene (PTFE), or can even be made from plastic or metal materials. Depending on their intended use, seals are classified into two groups, static or dynamic seals. Dynamic seals, such as rotary and reciprocating seals, play a pivotal role in applications involving moving parts, effectively serving as barriers between rotating shafts and moving pistons.

Dynamics seals are critical in both rotary and reciprocating equipment evidently displayed by the fact that they are often perceived as the component that experiences the most frequent failures. Despite their relatively lower cost when compared to the overall machinery, seals failure can potentially lead to costly downtime, contamination, and human health hazards. For instance, assuming a seal in an active rotary machinery fails, external contaminants such as seal's debris can enter the cavity, thus impacting the performance of the bearings that support the shaft under operational conditions. Such deterioration in bearing performance can provoke excessive shaft runout due to heightened vibration, which, in turn, is transmitted to other components in the machinery, resulting in expensive downtimes.

In various instances, replacing a seal post-failure can be exorbitant, meanwhile an early replacement of a seal may be inefficient by reducing the overall life utilization. Hence, assessing the beginning of the deterioration of rotary seals for informed maintenance decision-making is paramount. Existing literature primarily characterizes seal degradation by measuring physical properties. For instance, the impact of temperature, hydraulic oil, and compressive stress on seal degradation is assessed by measuring the chemical and mechanical properties of seal materials [1]. Another study focuses on characterizing the degradation of seals exposed to air at different temperatures under compression, using mechanical properties like weight loss, tensile strength, and elongation at break [2]. It is worth noting that various studies have shown that Tensile mechanical properties, volume swell, compression set, and chemical properties are measured to gauge seal degradation in hydraulic oil at various temperatures and immersion durations [3].

The the oil and gas industry has increasingly emphasized prognostics to enhance system utilization, safety, and reliability. Prognostics is an engineering discipline focused on foreseeing the point in time when a system or component will cease to fulfill its intended function. This

cessation of performance typically indicates a failure, rendering the system unable to meet the desired performance standards. Key aspects of prognostics include enhancing equipment availability by minimizing downtime, preventing catastrophic failures, improving the rate of return on equipment through predicting failures in advance, reducing operational risk for critical equipment, and enabling timely and informed maintenance decisions. Failure prognostics are commonly categorized into model-based and data-driven method [4].

Model-based prognostics, also known as physics-based or behavioral models, utilize algebraic and differential equations to represent system behavior, such as degradation, under various operating conditions, based on the laws of physics. For instance, a study mesured changes in material properties and seal performance using constant temperature oil bath to age the seals [5]. The performance of seals, characterized by leak and friction torque, was computed through numerical simulations employing a mixed Elastohydrodynamic (EHL) model. Similarly, the impact of heat and oxygen on changes in material properties and seal performance was investigated using an air oven aging test, with performance characteristics computed using a mixed EHL model [6].

Data-driven prognostic methods utilize artificial intelligence tools or statistical approaches to model system degradation and predict future health without relying on knowledge of the physics associated with the system. Studies demonstrated the success of data-driven prognostics in monitoring the health condition of bearings in rotating machinery through the use of accelerometers and vibration transmitters [7-9]. Since the failure of seals is a significant factor in bearing deterioration, developing a prognostics approach to monitor seal health is imperative.

The study of dynamic seals has been a focus of research since the 1950s, with numerous researchers exploring physics-based prognostic methods that involve estimating material,

mechanical, and seal properties [5, 6]. Monitoring the performance of seals during operation is particularly challenging for users due to the difficulty in tracking changes in physical parameters. Fortunately, the advances in sensor technology, wireless communication, and computational capabilities have brought about a significant transformation in the approach to monitoring the health of mechanical equipment and its components.

2.3 Rotary Seal

Rotating machinery is a largely used mechanical equipment in the oil and gas industry. It is a mechanical system comprised of hydraulic oil, sealing grooves, bearings, shafts, gear, and radial lip seals [10]. Failure of the radial lip seal is one of the primary causes of rotary machinery systems. In the oil and gas industry, lip seal failure can lead to significant repair time and substantial financial expenses, which is why the understanding of its performance evaluation under testing conditions is paramount.

The rotary lip seal encompasses an elastomeric lip and the shaft, and it is affixed to the rotary shaft through an interference fit. In Figure 1, the cross-sectional view illustrates the elastomeric lip situated on the rotary shaft. The sealing edge of the elastomeric lip is pressed against the counterface surface of the shaft, forming the crucial functional region of a rotary seal.

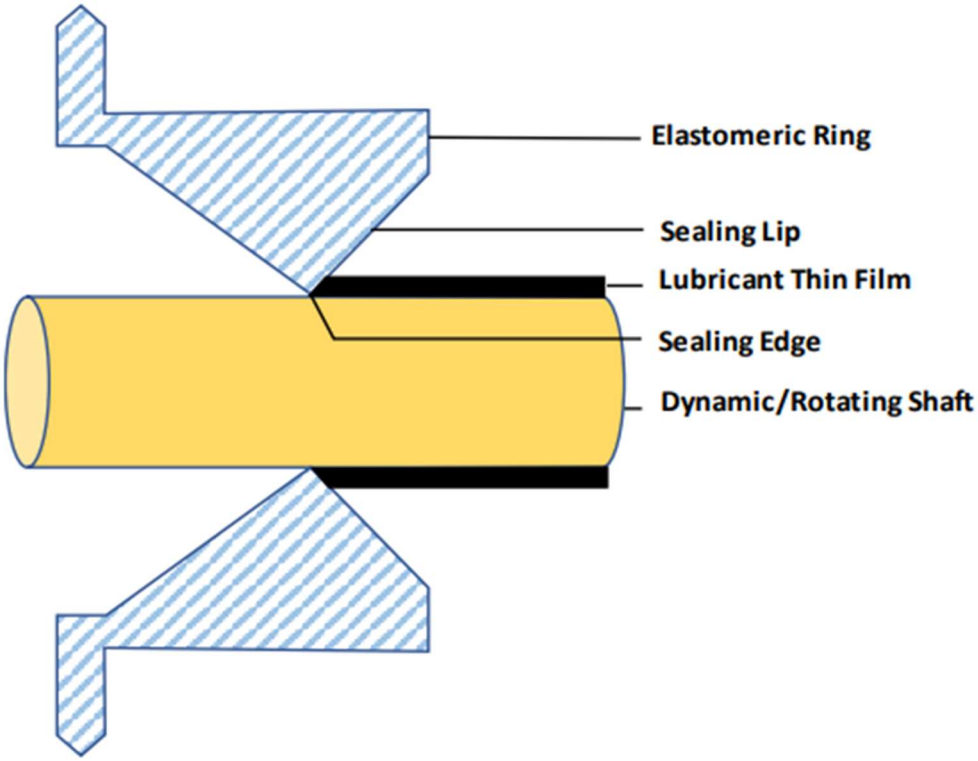


Figure 1: Cross-section of an elastomeric lip on a rotary shaft [10]

Incorporating a spring serves primarily to maintain a steady pressure on the shaft over the seal's lifespan. Additionally, it assists in ensuring continuous contact between the lip and the shaft, particularly at elevated shaft speeds, and helps counteract compression set and wear on the lip material. Various types of springs are employed to energize the lip, such as garter or wound springs, cantilever springs, canted-coil springs, and helical coil springs, each offering distinct characteristics based on their displacement-to-load ratio [10]. Yet the rotary seal itself is only one component of the mechanical seal that is subject to interest.

2.4 Mechanical Seal

A mechanical seal is widely known as a dynamic sealing mechanism, featuring flat radial surfaces, a stationary one and rotating others, pressed together by a combination of system

pressure and a spring force [11]. The stationary part of the seal can be precisely located within a housing where the rotating part is typically spring-loaded and free to move along the shaft, thus accommodating system misalignments while providing proper sealing contact [11]. Mechanical seals have become more demanding and are currently the primary choice for containing fluids in a dynamic sealing application involving a rotating shaft like centrifugal pumps, mixers, and compressors [11].

Mechanical seals are classified based on the load to the sealing surfaces and around the rotating shaft, with the latter often referred to as secondary sealing [12]. There are three categories of seals, namely elastomer-bellow seals, pusher seals, and metal-bellow seals. Elastomer-bellow and pusher seals utilize a metal spring to generate contact pressure at the sealing interface. In pusher seals, an O-ring forms the secondary seal, as opposed to the elastomer-bellow seals, where the elastomer below itself serves as the secondary seal [11] . The pusher and elastomer below seal are similar in the sense that they are both comprised of a main spring seal and a secondary seal, unlike the metal-below seal. However, metal-bellow seals offer the advantage of the bellow acting as both the spring and the secondary seal around the shaft [11]. Similarities between the pusher and elastomer-below seals could be seen by their respective nomenclature as detailed in Figure 2.

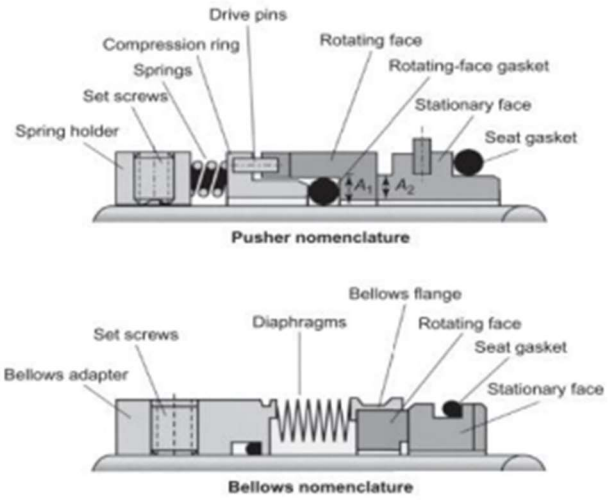


Figure 2: Mechanical seal nomenclature [11]

A pusher seal is generally comprised of a stationary face, a rotating face, and additional elements such as gaskets, drive pins, springs, and spring holders, which are adjusted to suit operational requirements [11]. In many designs of pusher seals, the stationary seal is affixed to the housing using a retaining ring and pin, while the rotating face is allowed axial movement but is secured in place by a spring and spring holder. The gasket on the rotating face is often termed a dynamic secondary seal or simply a secondary seal because the rotating part of the mechanical seal can move axially. Despite a plethora of materials at disposition, dynamic secondary seals are commonly made of elastomer with pressure and temperature restrictions. Additionally, the spring holder regulates the compression of the spring, thereby generating the contact pressure at the sealing interface [11, 12].

Metal-bellow diverges from pusher seals as it functions as the spring responsible for creating contact pressure at the interface [11]. Unlike conventional springs, a metal bellow can also prevent fluid flow and sustain pressure. This feature allows for the integration of the secondary seal into the bellows adapter, which prohibits axial movement and establishes a static

seal [11]. Metal-bellow is typically welded or hydroformed into place, eliminating the need for drive pins to transmit torque from the shaft to the rotating face of the mechanical seal [11]. Each seal has its advantages and disadvantages. In the case of the metal-bellow, its static secondary is suitable for higher temperatures and a wider range of fluid types due to greater material options, design and geometry [11, 12].

Elastomer-bellow is evidently made of elastomer and replaces the spring responsible for creating contact pressure at the interface. In certain instances, the elastomer-bellow serves as the static secondary seal, transfers torque from the rotating shaft to the seal face, and offers the necessary system flexibility for misalignment. However, unlike metal bellows, elastomer bellows lack the capability to exert the axial force needed at the sealing interface. Therefore, a spring is necessary to maintain contact pressure, similar to a pusher seal. The elastomer-bellow seal is attractive because the rubber bellow provides a static secondary seal, whereas pusher seals, for instance, rely on a dynamic secondary seal.

These seals are all similar in concept and usage but differ in design. The major difference revolves around the contact pressure at the sealing interface. The pusher seal utilizes a spring holder to create the contact pressure at the sealing interface, while the metal-bellow and elastomer seal perform the functions of the spring in the pusher seal. Many more types of mechanical seals are being developed. There is no perfect or best mechanical seal. The ideal mechanical seal to use is largely based on the specific application of and testing conditions of the experiment.

Chapter 3: Experimental Steup

3.1 Introduction

This chapter provides a detailed overview of the rotating seal testing system and also offers concise instructions for using and troubleshooting the system during experiments. The following section will dive into the specificities of the Device Under Testing (DUT), volume displacement, the pressure sensors and temperature, motor, controller, and test chamber rotation.

The testing system is a setup designed and implimented by former students with the center piece being a Device Under Testing (DUT) provided by industry partner. The testing system is also referred as 10K-RPM rig or 10K for its ability to operate up to a speed for 10,000 rpm. More on the testing conditions on the next chapter.

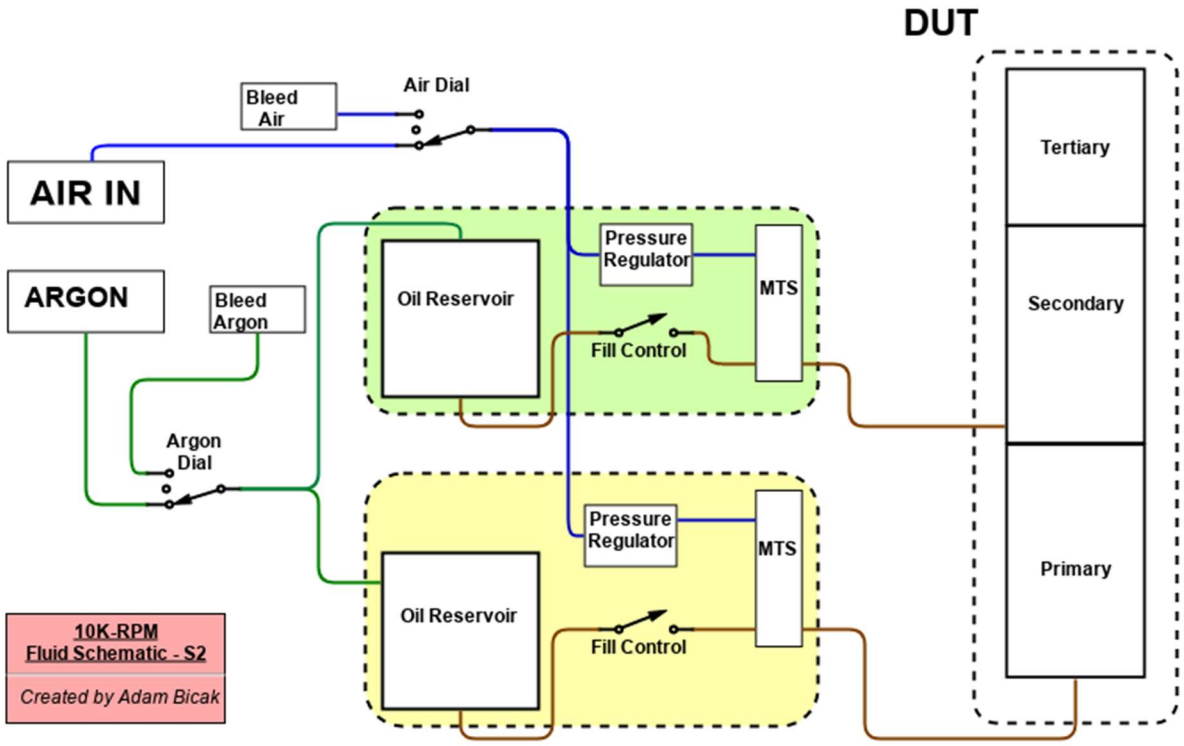


Figure 3: Fluid schematic of the 10K- RPM rig [13]

The fluid schematic displays an overview of the entire mechanical system as indicated in Figure 3. It is comprised of 2 oil reservoirs, argon and air gas intakes, two bleeding controllers, two MTS sensors and pressure regulators and the DUT itself comprised of three chambers. The 10K system possesses the ability to gauge volumetric displacement between two sealing surfaces, as well as measure pressure from both reservoirs through the MTS sensors. Additionally, it can monitor temperature at multiple points of interest through thermocouple probes. The oil reservoirs are connected respectively to the primary chamber, and the other one for the secondary and tertiary chambers. The primary oil reservoir is often mixed with a color dye in order to estimate the amount of oil leaked to the secondary and tertiary chambers. Argon gas is responsible for pumping oil through the MTS sensors all the way to the respective

chambers. Air gas seats on top of the piston inside the MTS sensors and are regulated by the pressure regulators. The argon and air are regulated with a control panel. More on that in the following sections.

3.2 Modules with same parameters

3.2.1 MTS and LVDT sensors

In order to better understand an MTS sensor it is necessary to understand the function and principles of the LVDT sensor as they go hand in hand. The Linear Variable Differential Transformer (LVDT) sensor comprises a thin rod with a magnetic ring that can move along it without constraint. The LVDT output from the MTS sensor provides a constant voltage signal corresponding to the linear displacement of the transducer, which determines the volume within the primary chamber. This voltage signal changes based on the transducer's position alterations, facilitating volume change calculations as it shifts. A valve and pressure regulator connect the upper chamber of the MTS sensor to the compressed air supply. This upper chamber pressurizes the lower chamber of the MTS sensor by applying force to the piston head. The lower chamber, filled with oil, links to the Device Under Testing (DUT). The hydrostatic pressure within the lower chamber transfers to the DUT, ensuring the primary chamber (Chamber 1) remains pressurized. Inside the MTS sensor, there is a piston separating the space into two chambers. This piston encases the magnetic ring monitored by the LVDT sensor. By tracking the movement of the piston along the LVDT shaft, it's possible to calculate the volume change in each chamber. This calculation is based on the known diameter of the fluid volume cylinder and the height of the piston head. Figure 4 shows a schematic of the operating principle and an actual picture of the MTS sensor.

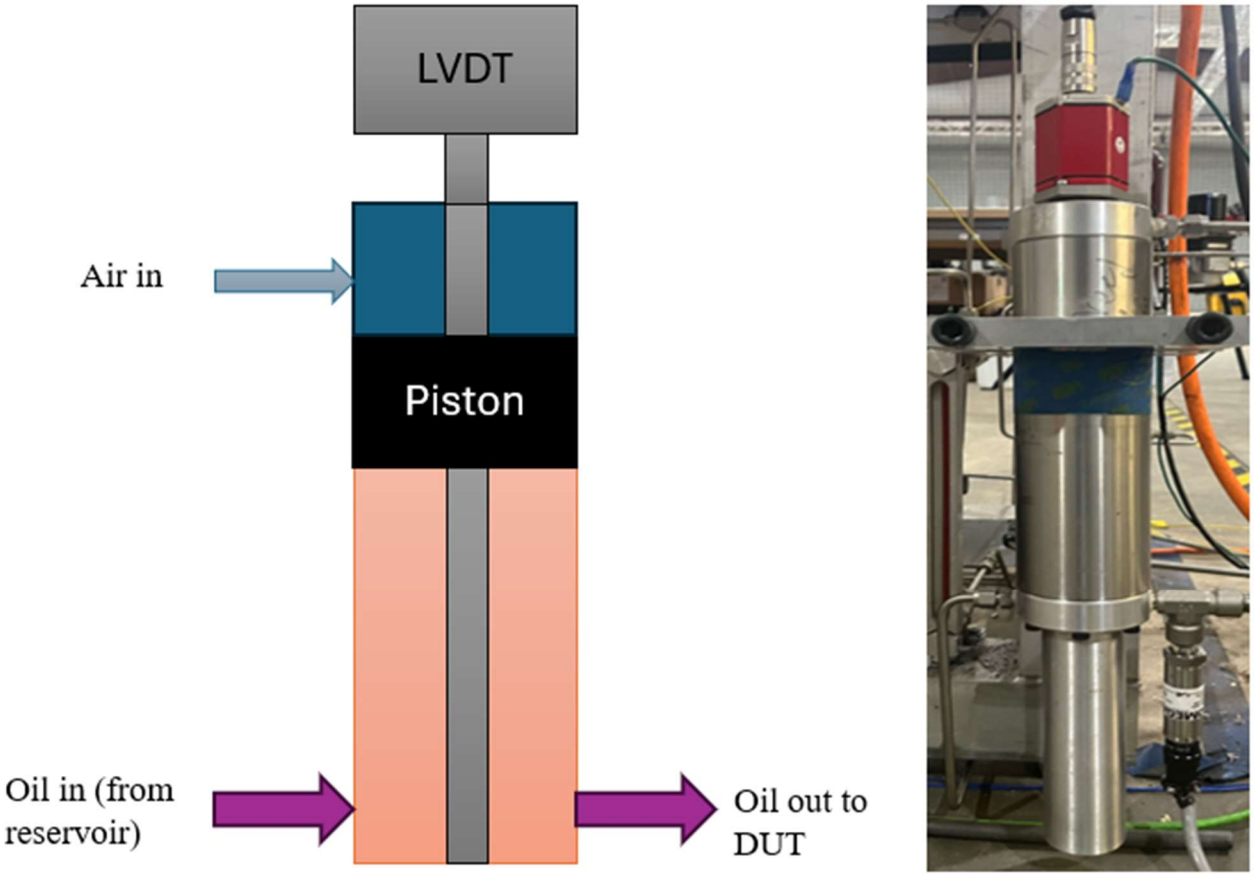


Figure 4: MTS sensor schematic

The volume displacement sensor comprises five distinct parts: the piston housing, hydraulic side endcap, sensor side endcap, piston, and MTS sensor. Below is Figure 5, illustrating the arrangement and positioning of these components in the assembly as well as the entry and exit points of oil respectively from the reservoir and to the test chambers of the DUT.

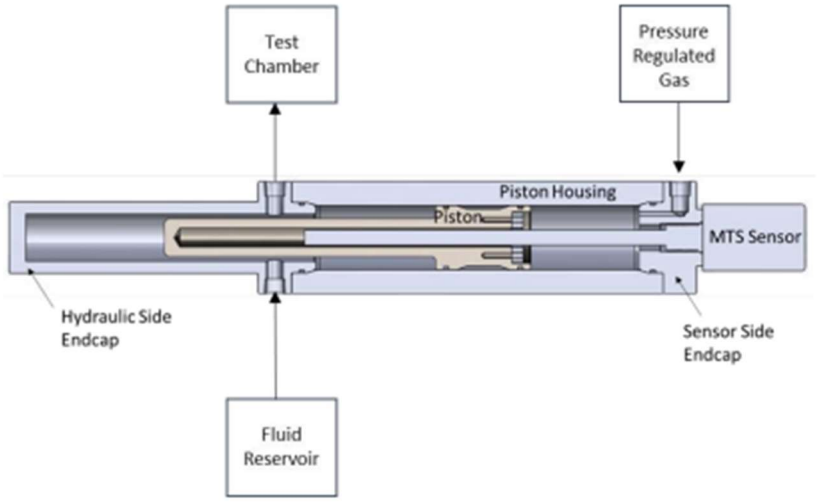


Figure 5: Schematic of the components of the MTS sensor [12]

Analyzing the schematics of Figures 4 and 5 exhibit the pressurized argon and air gases entry points to the system through two quick disconnect pipes situated near the controller, enabling pressurization of both the tanks and the primary chamber. The air flow is regulated by a pressure regulator to maintain desired pressure levels within the system. It is then directed to the upper chamber of the MTS sensor, exerting downward force on the piston head to pressurize the lower chamber. This lower chamber is linked to both the oil tank and the DUT. The hydrostatic pressure within the lower chamber is transferred to the DUT, ensuring continuous pressurization of the primary chamber.

3.2.3 DUT

The DUT, denoting Device Under Testing, is a cylindrical assembly provided by industry partner. This assembly features three chambers: "Primary," "Secondary," and "Tertiary," each separated by a sleeve referred to as a seal body, which accommodates a friction seal. Positioned at the concentric center of the DUT is a lengthy rotating shaft extending from top to bottom.

Within the primary chamber of the DUT sits a thrust bearing assembly, affixed to the rotating shaft at the bottom.

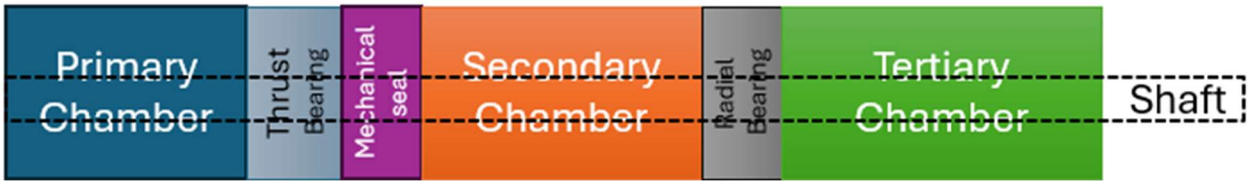


Figure 6: Simplified schematic of the DUT

Figure 6 exhibits the schematic for all 3 chambers of the DUT, including the attached shaft from the thrust bearing. The main seal, often the only one, is positioned between the primary and the secondary chambers. The primary chamber is pressurized while the secondary and tertiary chambers will be at atmospheric pressure.

The exterior of the DUT features multiple ports and threaded sockets, providing the means to mount thermocouples, pressure transducers, and proximity probes to facilitate data collection. Figure 7 illustrates the location and nomenclature of the thermocouples, pressure transducers, and journal bearings.

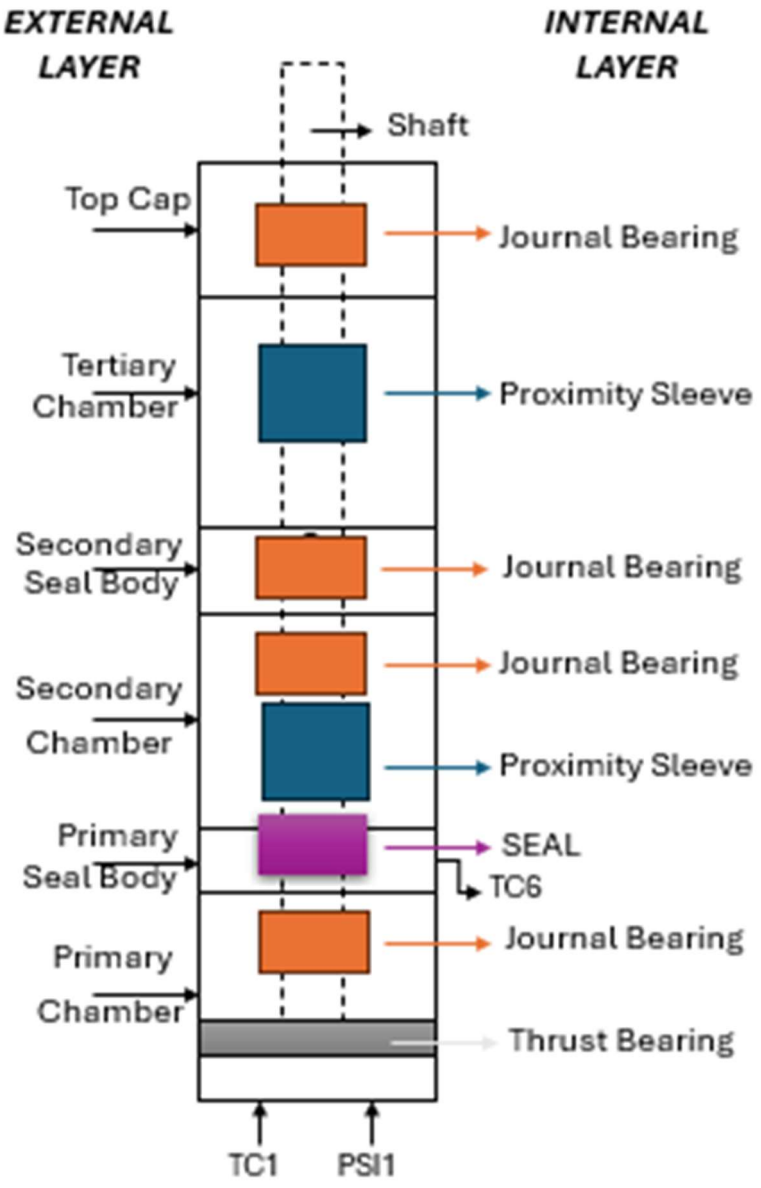


Figure 7: Detailed DUT nomenclature

3.3 Modules with different parameters

3.3.1 Motor

The motor is tasked with rotating the shaft traversing the DUT and is powered by 480-volt 3-phase electricity. During an experiment, the motor is rotated to the vertical position for the entire duration of the experiment at a maximum operating speed of 10,000 rpm. Attached to the

motor is the coupler as indicated in Figure 8 below. The coupler connects the motor to the DUT shaft.

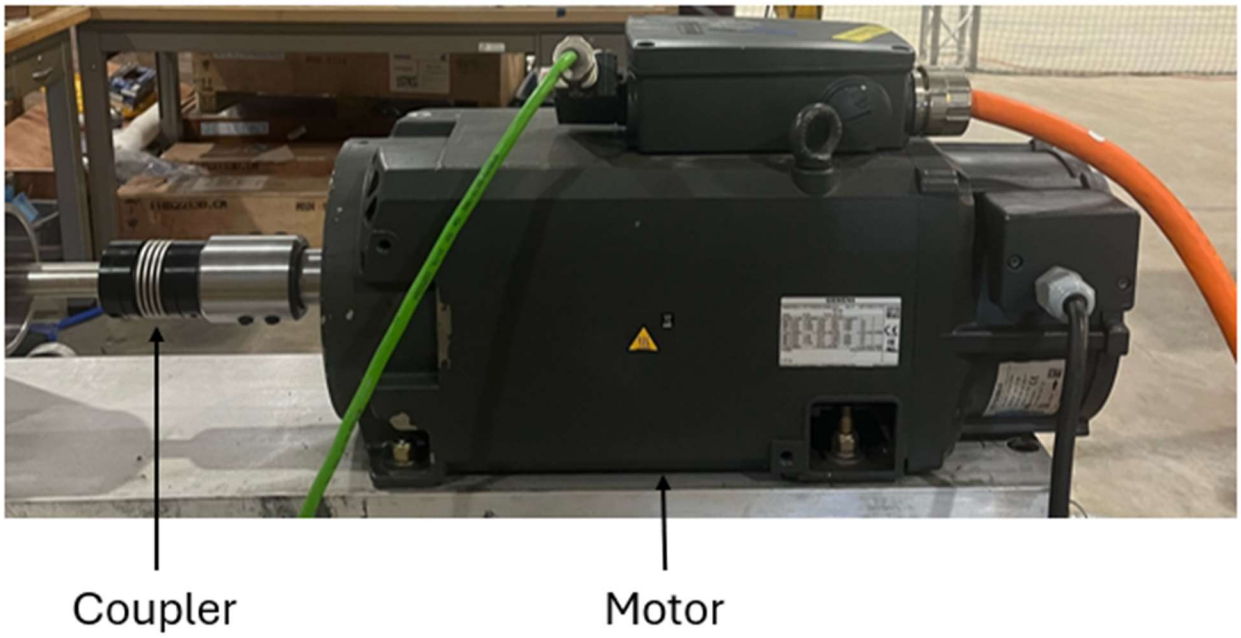


Figure 8: Motor on the horizontal position

3.4 Other Components of the Systems

3.4.5 Argon and Compressed Air Gases

The testing system utilizes two distinct gases throughout its operations, each serving specific functions. The argon tank, functioning as an inert gas source, plays a pivotal role in facilitating the movement of liquid oil from the oil reservoir to both the MTS and the DUT chambers. The inert nature of argon is crucial, preventing any chemical reactions and subsequent oxidation within the DUT during testing, a risk that a non-inert gas would pose.

Conversely, compressed air, as seen below, is sourced from a sizable air compressor tank and undergoes filtration to eliminate moisture content. This purified compressed air serves a

singular purpose: applying pressure to the MTS sensors, positioned atop the piston head as illustrated in Figure 4.



Figure 9: Compressed air supply

3.4.1 Control Panel and P.I.D controller

The control panel is comprised of four dial and two P.I.D controllers. Figure 10 presents an authentic look of the control panel.

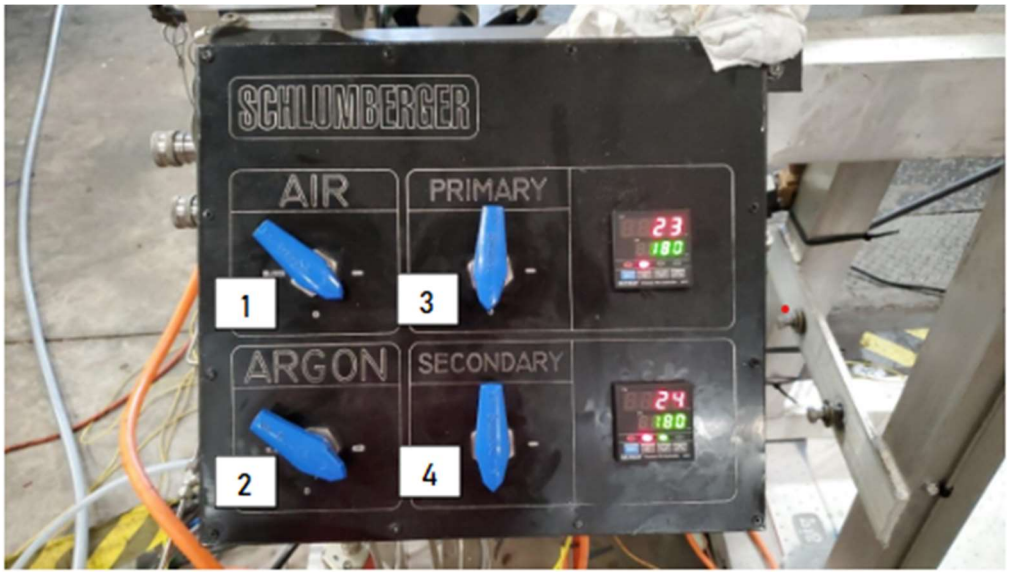


Figure 10: Control panel for 10K system [13]

The above dials on the control panel are numbered to further detail the use of each one of them. Dial 1 regulates the flow of compressed air into the 10K, offering three settings: Bleed, Cutoff, and Open. Bleed depressurizes the system for regulator adjustments, Open allows air in, and Cutoff stops air supply to the 10K without releasing air from the system. Dial 2 manages argon flow into the test stand's oil reservoirs, featuring Bleed, Cutoff, and Open positions, mirroring Dial 1's functions. Dial 3 and 4, respectively, facilitate oil transfer from the reservoir to the DUT primary and secondary chamber with the same functions as Dial 1 and 2.

The control panel incorporates two PID controllers designed to regulate the temperatures of both the primary and secondary seal bodies. Each PID controller is equipped with dual screens, one displaying the temperature setpoint and the other indicating the current temperature. The controller regulates the inside temperature of the DUT chambers. The system operates at a set testing temperature and when exceeded, the PID controllers regulate the temperature down to the desired temperature by heat transfer process through the cooling system.

3.4.2 Cooling system

During high speed-rotation tests, the oil inside the chambers overheats and expands. To combat this phenomenon a temperature control mechanism, mostly known as cooling system, is used to maintain the desired temperature within the range of the experiment. The cooling mechanism prevents the temperature from surpassing the maximum allowable temperature of 200°C (392 ºF) during high-speed rotation. This is facilitated through a PID-controlled cooling system, which triggers when the system surpasses 180°C. Two cooling systems were used, and both followed the same mechanism. They each regulate the temperatures through conduction and convection heat transfer by having running water flow through an entry point and eject the substantially hot water through a different exit point. The cooling system is automatically activated through the PID controller when needed. This allows the test to be performed at a set temperature regardless of the rotated speed of the DUT.



Figure 11: Schematic of cooling blocks

Figure 11 shows the first cooling system, also known as cooling block. The cooling block refers to a collection of aluminum heatsinks designed for liquid cooling, which are affixed to the exterior of both the Primary and Secondary seal bodies during experimental procedures as can be seen above.

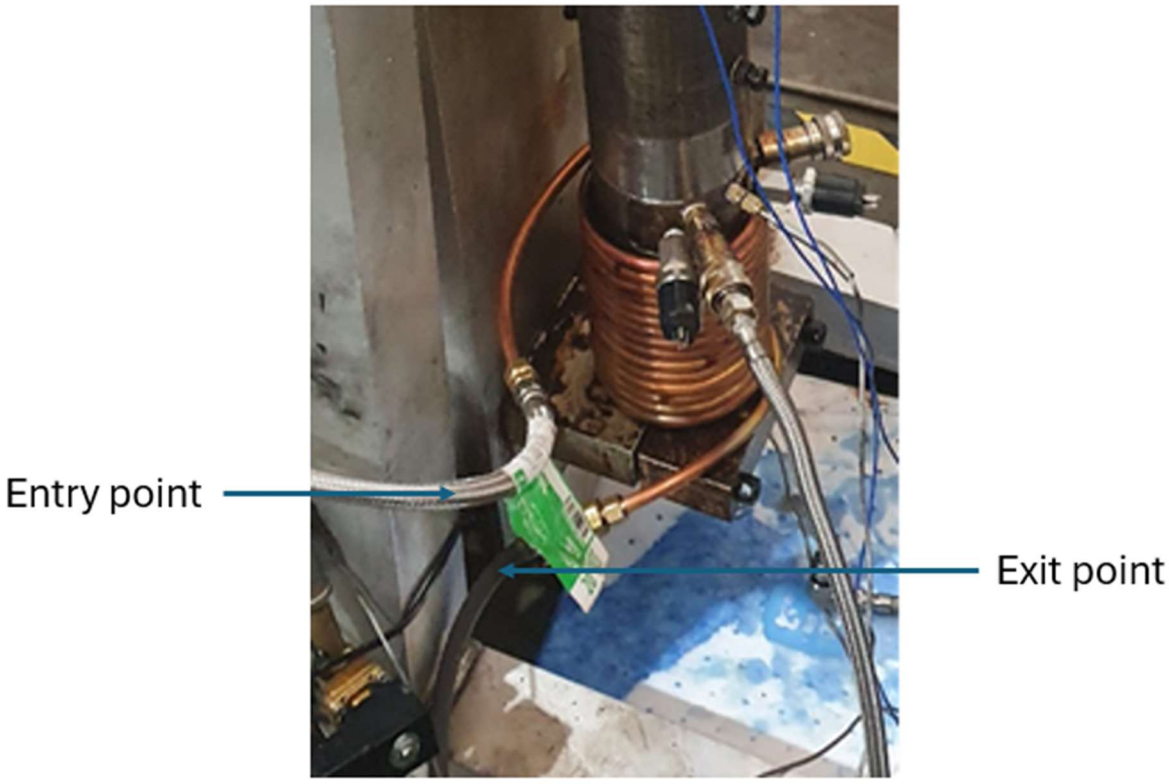


Figure 12: Copper cooling wire loop

Figure 12 shows the first cooling system. The cooling system is made of a copper pipe coiled around the Primary chamber of the DUT during experiments which regulates water flow using PID controllers on the Control Panel. Room temperature water is pushed through the copper wire loop from one end to another when the temperature of the Primary seal body surpasses the setpoint on the PID controller.

3.4.3 Test Stand

The Test Stand is made of three primary components: the frame, the tabletop assembly and the rotating mechanism. The Test Stand is predominantly constructed from aluminum to facilitate manufacturing and assembly processes. It has the ability to pivot and hold the DUT in

the vertical position. Figure 13 illustrates the test stand and its components in the horizontal position.

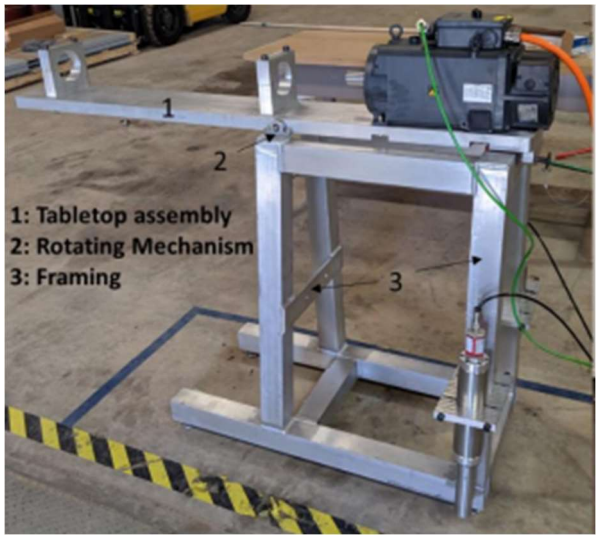


Figure 13: Test stand [12]

3.4.4 Vacuum Pump

Each Tests requires new oil for mechanical and results purpose. To do so, the previously used oil trapped inside the DUT chambers must first be removed from the pressurized chambers using a vacuum pump. Figure 14 shows a portable electric vacuum pump used to effectively extract fluid from the interior of the DUT.



Figure 14: Vacuum pump

The vacuum pump connects to each chamber to remove used fluid. Figure 15 shown below, illustrates the vacuum pump schematic on DUT used to remove used fluid. Figure 15 also shows the fluid reservoir schematic during testing. To avoid pressurizing the fluid reservoir, as it could introduce gas pockets due to intricate seals and bearings, leading to fluid degradation and sludge formation, the valves connecting the fluid reservoir to the test chambers remain closed.

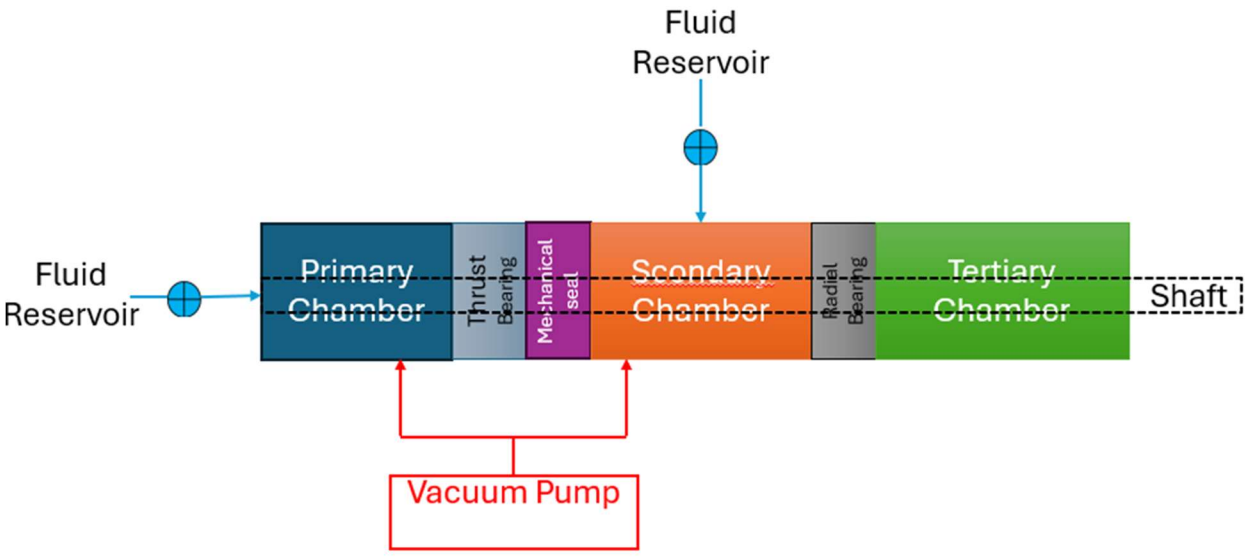


Figure 15: Vacuum pump schematic on DUT

3.4.6 Complete Mechanical Test System

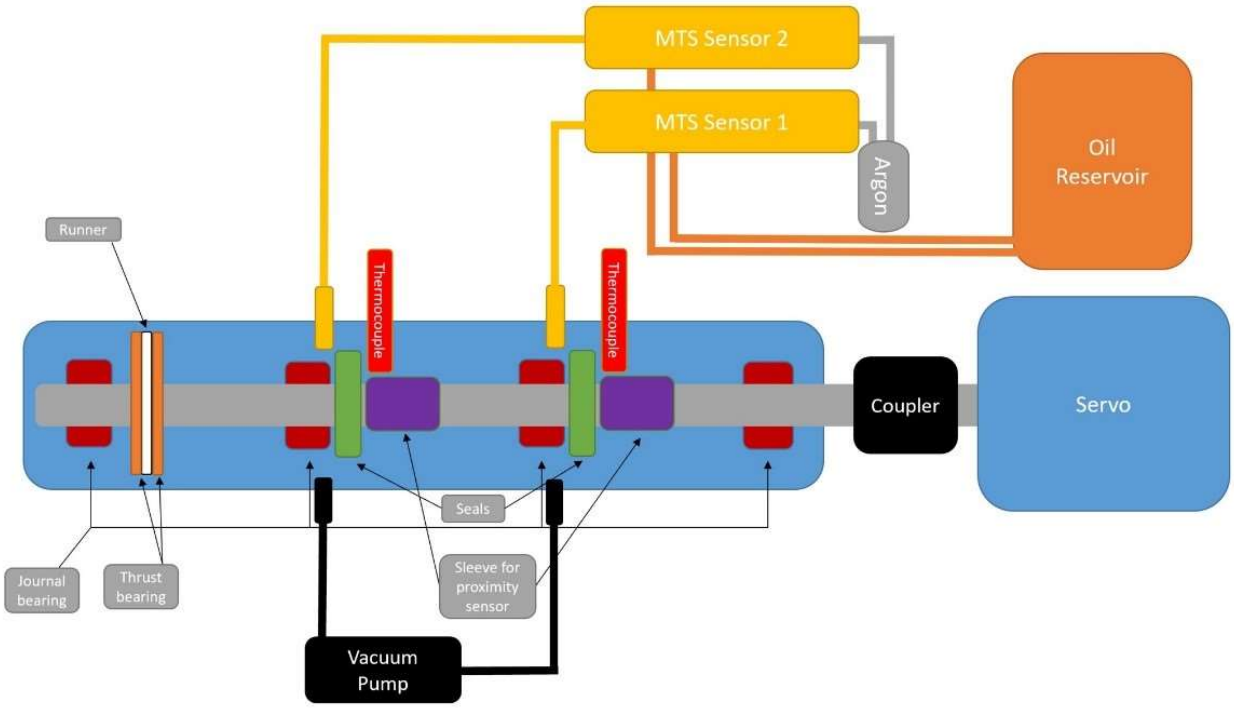


Figure 16: Complete mechanical schematic of the test system [14]

Figure 16 shows the complete mechanical schematic of the 10K test system. It can be seen that the supply oil reservoir pumps the oil through the Volume Displacement Measurement Device, also known as MTS sensors, into the test chambers. Highlighted in black are the schematic of the vacuum pump connected to the DUT and the spring collar. The DUT shaft is attached to the electric motor through a spring collar also known as coupler. The primary purpose of the spring coupling is to connect the shaft to the electric motor but as importantly to absorb any torsion and shear stress in case of misalignment or rotation failure. Frequent failures associated with such events will result in a breaking of the spring collar.

3.4 Assembly

Before testing, it is paramount to have a correct setup of the DUT. The First step is hooking the primary chamber DUT and the attached rotating shaft to the workbench, where the DUT can be fully mounted. Next goes in the seal. The seal is set up between the primary and secondary chambers, with distinctive installation procedures varying based on the type of seal used and the manufacturer's instructions. Figure 17 shows the primary chamber and rotating shaft mounted on the workbench.



Figure 17: Workbench and primary DUT chamber

The following steps consist of attaching respectfully the secondary chamber, the tertiary chamber and the top cap. Figure 18 presents a fully assembled DUT model on a workbench.



Figure 18: Fully mounted DUT

After assembly, the DUT is mounted on the test system test stand in the vertical position. It is in this position that all thermocouples and pressure sensors are attached to the DUT, same as the DUT shaft to the servo motor through the spring collar. Figure 19 illustrates the DUT connection to the servo motor and test stand in the vertical position.

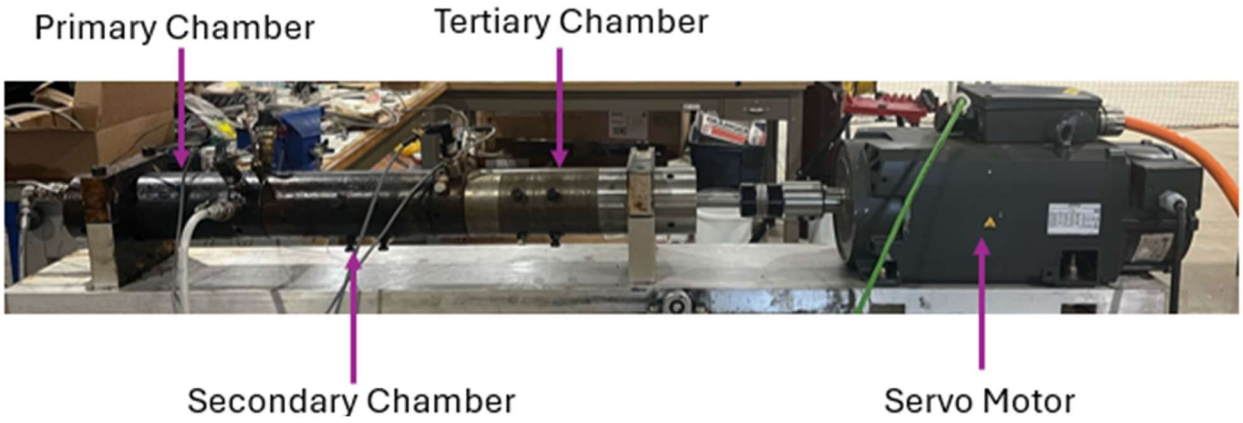


Figure 19: Fully mounted DUT attached to the motor

Once the DUT is safely attached to the servo motor it is ready to be set in the testing position. The test stand is thus rotated from the horizontal position to the vertical position through the pivot point using a pulley system that is associated with the frame as Figure 20 indicates below. Figure 20 shows the test stand in the testing position and the location of the pulley system used to safely pivot the test stand in the vertical position. The stand is secured into the testing position using bolts locking the stand to the frame.

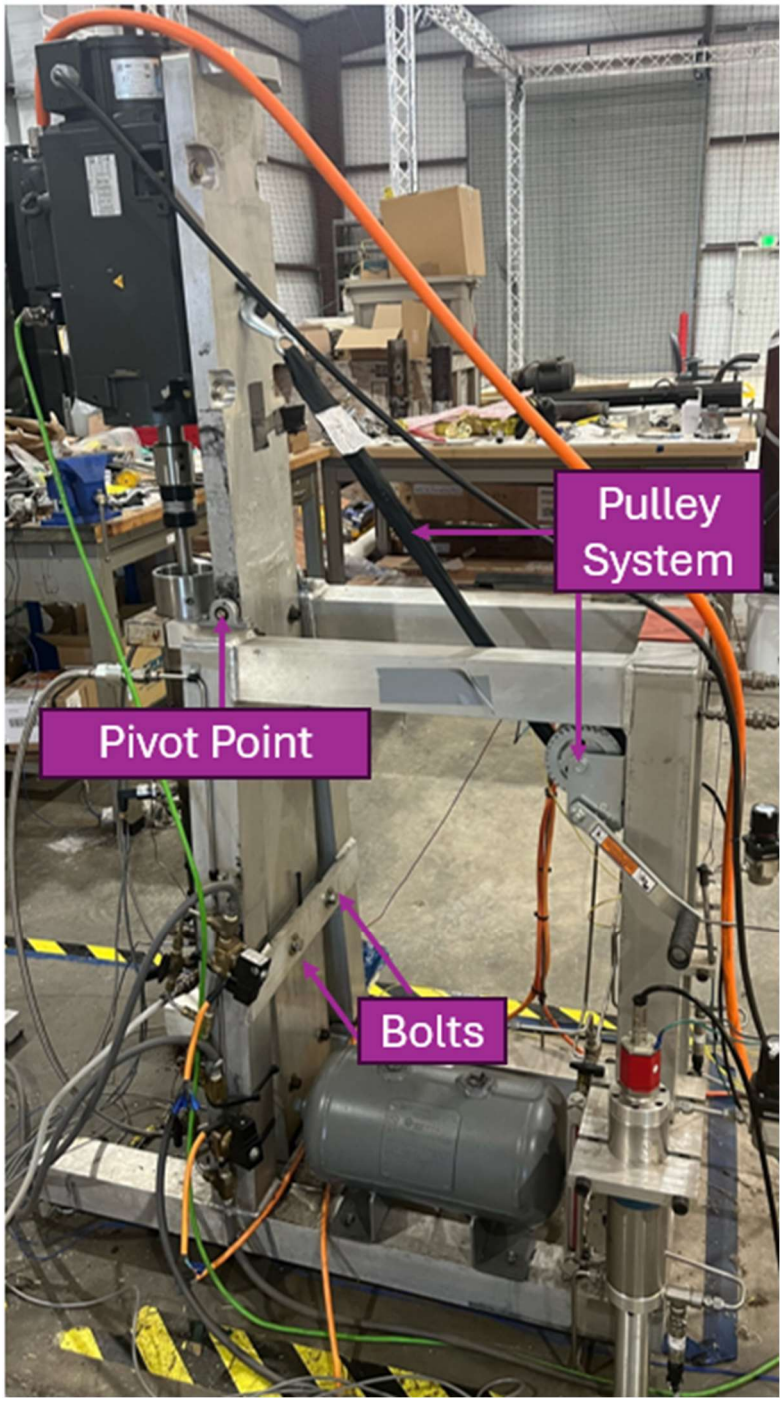


Figure 20: Testing system on the vertical position

3.6 Data Acquisition and Processing

3.6.1 User Interface (LABVIEW)

Numerous instruments are employed for acquiring data, capturing temperature, pressure, and volume in both primary and secondary regions of the DUT. These instruments are managed and monitored through LABVIEW user interface, connected to multiple NI DAQ controllers and other components. The user interface shows temperature, pressure, and volume displacement readings obtained from the sensor, and also enables the user to record sensor data as seen in Figure 21. The LABVIEW program is equipped with safety measures programmed to halt the rotation of the servo motor when temperature values exceed a specific threshold.

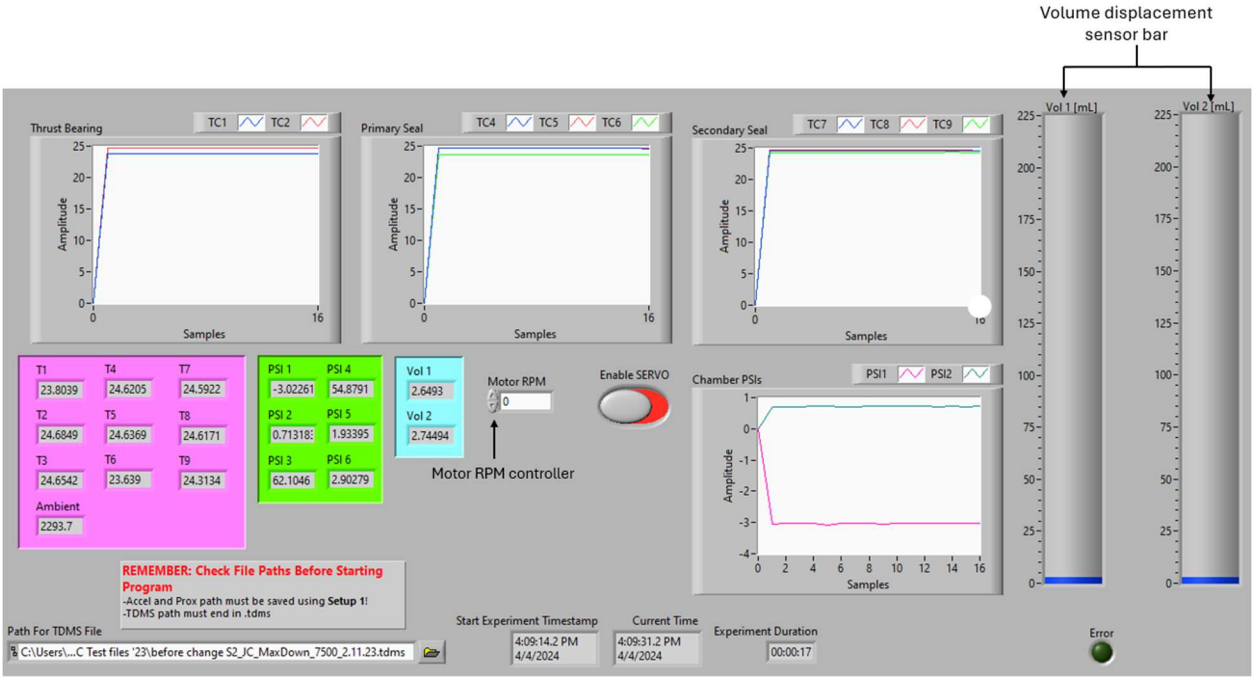


Figure 21: LABVIEW user interface

. The temperature is monitored using thermocouples installed in the bottom cap, primary, and secondary seal bodies. Volume is measured using an MTS sensor equipped with a linear variable

differential transducer, while pressure readings are obtained from pressure transducers threaded into the seal bodies. LABVIEW collaborates with the PID Controller to automate system control or respond to inputs within the interface. Motor speed is adjustable and visualized through graphs displaying various points in the DUT, programmed to specific RPMs based on voltage outputs. Data is stored in a tdms file format for analysis in MATLAB. The system operates based on a block diagram established by the original designers, maintaining its integrity due to interdependent functions.

3.6.2 Matlab

Once the data is collected through the LABVIEW user interface, it must then be processed into visual graphs for analysis. To do such things, the TDMS Excel sheet containing the data is first saved as a Tab-delimited (.txt) file, thus ensuring the file name is devoid of spaces and special characters. The text document is then placed in the Workspace folder accessed by the MATLAB instance. Next, within the data processing program, the file name variable is modified to match the name of the file such as ‘file_name.txt'. If the data is too heavy to be processed or has multiple redundancies in the graph, the data can then be downsampled for easier analysis. When downsampled, the program must be adjusted on line 40 of the code accordingly in the MATLAB code to correct the timescale displayed.

The program is then executed to generate graphs. The generated graphs, from top to bottom, represent the following data from the primary chamber: temperature (TC6), Pressure (PSI1), and Volume (Vol1), with the time scale measured in hours.

Chapter 4: Leak Rate Analysis

This chapter is divided into four sections. The first section details the calculation of leak rates and outlines the testing conditions. The second section examines the leak rate performance of a mechanical seal tested under the manufacturer's specified conditions at ten thousand (10,000) RPM. In contrast, the third section investigates the performance of a seal subjected to operating conditions beyond those recommended by the manufacturer. The fourth section identifies and analyzes the root causes of common testing failures utilizing experimental data.

4.1 Leak rate calculation and testing conditions

The testing conditions for experiments are monitored through LabVIEW throughout the duration. The tests are conducted under constant temperature and pressure inside the primary chamber as they can directly impact the efficiency of the seal and, consequently, the leak rate. All tests are performed at the same temperature and pressure conditions in order to have data uniformity and accuracy in the evaluation of the leak rate. The primary chamber is maintained at a temperature of 180°C $\pm$ 3°C and pressure of 15 psi $\pm$ 3 psi.

The leak is estimated by performing slope calculations in steady state of the collected data. Once the experiment is started, it takes time for the temperature and pressure to stabilize. The stabilization period is the time given for the temperature and pressure to reach the desired values of 180°C and 15 psi respectively. This stabilization period is reflected through unstable volume change in primary chamber lasting anywhere from half an hour to five hours. Data collected during the stabilization period are not used for leak rate calculation. The end of the stabilization period also marks the first point of the two-point slope used to determine the leak rate called the estimated stabilization point.

The stabilization point selected marks the end of the stabilization period and the beginning of the linear volume leak in the primary chamber (chamber 1). Together with the end point they construct what is known to be a leak rate zone, where the leak rate is evaluated. The end point is the last data point before another stabilization period or an abrupt ending due to failure. Figure 22 illustrates a volume leak rate of a seal indicating the stabilization period, the estimated start and end points, and the leak rate zone evaluated highlighted in red.

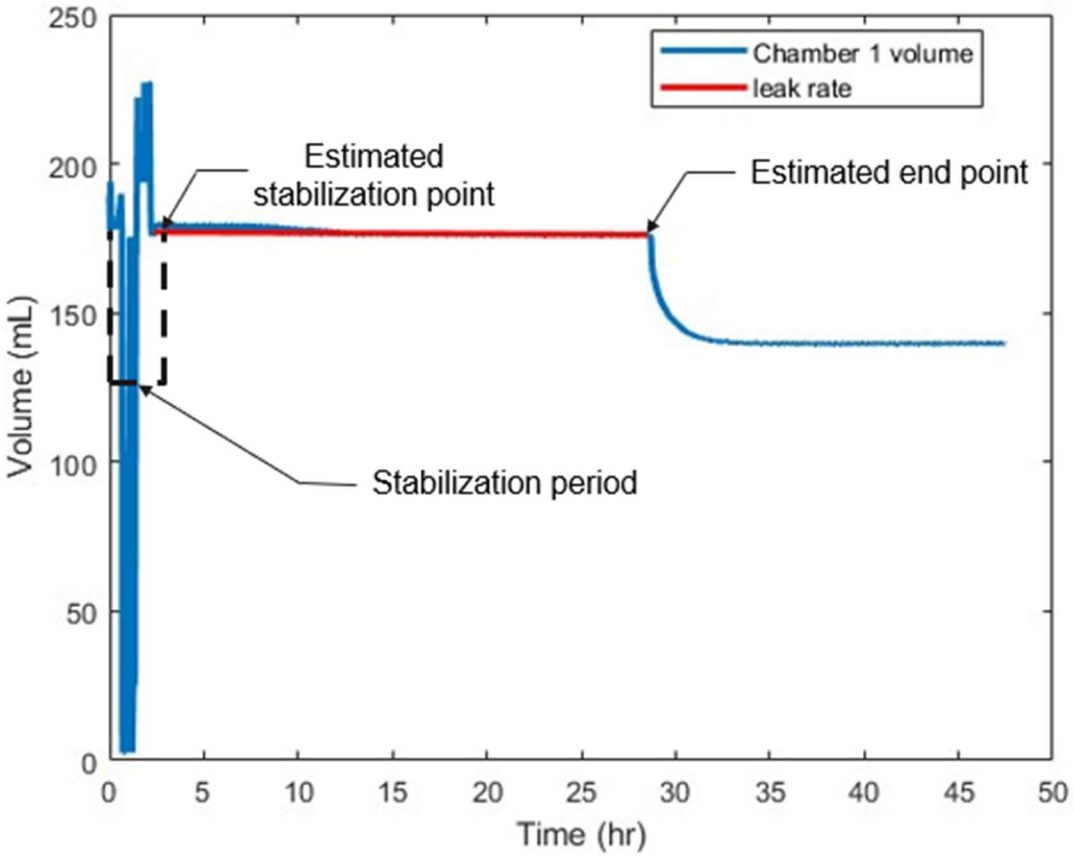


Figure 22: Volume leak rate of a seal showing stabilization period with estimated start and end points

The leak rate is calculated from a slope equation between the stabilization point and the end point. Let the stabilization point have the coordinates (x_1, y_1) and the end point the

coordinates (x_2, y_2), with the *x-abscise* representing the time coordinates in hours (hr) and the *y-abscise* representing the volume coordinates in milliliters (mL). The slope (m) in equation (1) representing the leak rate in the primary chamber through the seal is determined by:

$$m = \frac{y_2 - y_1}{x_2 - x_1} \quad (1)$$

For Instance, in Figure 22 the coordinates for the stabilization point and the end point are respectively (3.29, 175.8) and (28.32, 179.9). The total volume lost is thus 4.1 ml over a period of 25.03 hours. In this case following equation (2) the leak rate is calculated to be:

$$m = \frac{(179.9 - 175.8)mL}{(28.32 - 3.29)hr} = 0.163\ mL/hr$$

The leak rate in the case above is then estimated to be 0.163 mL/hr. This equation will be used to determine the leak rate for every data collected in the chapter.

While determining the leak rate, only stable and steady leak rate zones are analyzed as they are often unstable period due to drastic weather and temperature change. These zones are called neglected leak rate zones.

4.2 Leak rate of individual seals

This section evaluates the leak rate and discusses the results for an individual seal. The seal is evaluated by analyzing the volume leak rate through the seal from the primary chamber to the secondary and tertiary chambers. The seal is tested within the manufacturer specified speed at 10000 RPM with testing temperatures of 180°C $\pm$ 3°C and pressure of 15 psi $\pm$ 3 psi in the primary chamber.

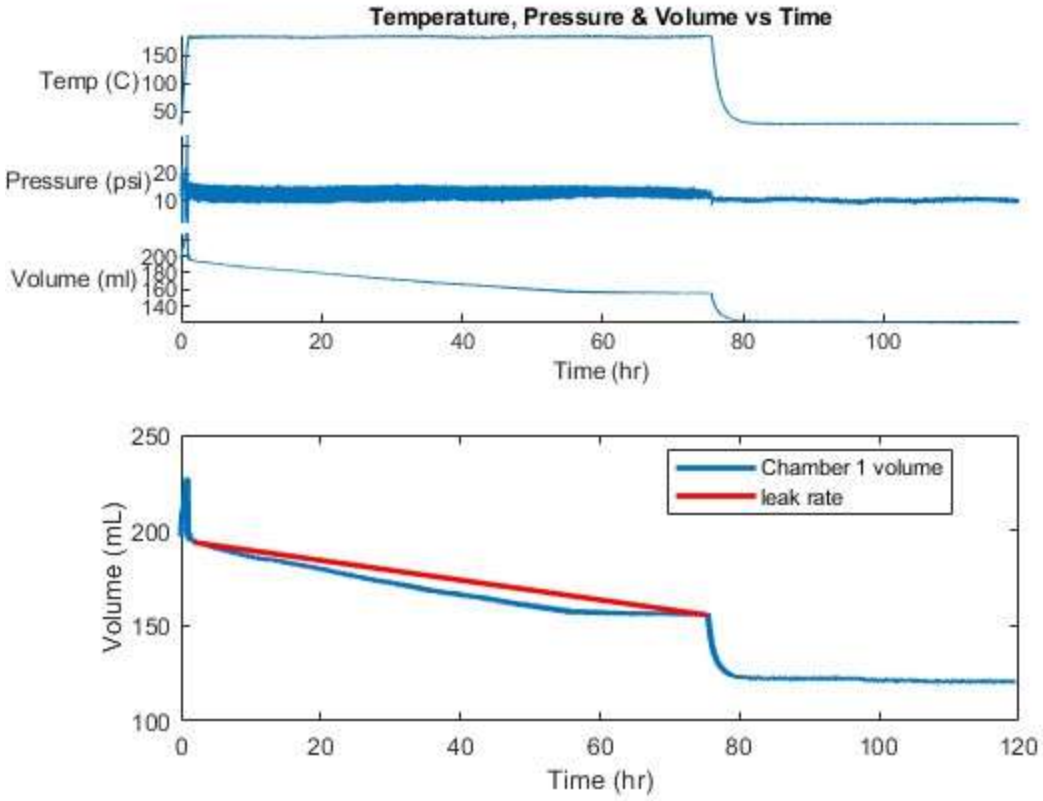


Figure 23: 75 hours leak rate at 10,000 RPM

Figure 23 shows the leak rate of a seal within manufacturer testing range at 10,000 RPM. The graph shows a seal test experiment with a leak rate data for 75 hours before abrupt interruption. The leak rate is calculated to be approximately 0.5497 mL/hr. A deeper look at the volume loss from Figure 23 shows that the leak rate seems to decrease significantly past 50 hours of data collected. This graph being insufficient to come to a realistic conclusion, another experiment is conducted on the same seal.

Figure 24 shows the repeated seal experiment for an additional 25-hour period ending with the same system failure as the experiment above. Yet this time, chamber 1 experiences a total volume loss of 4.1mL over a span of 25.03 hours bringing the leak rate to be 0.163 mL/hr.

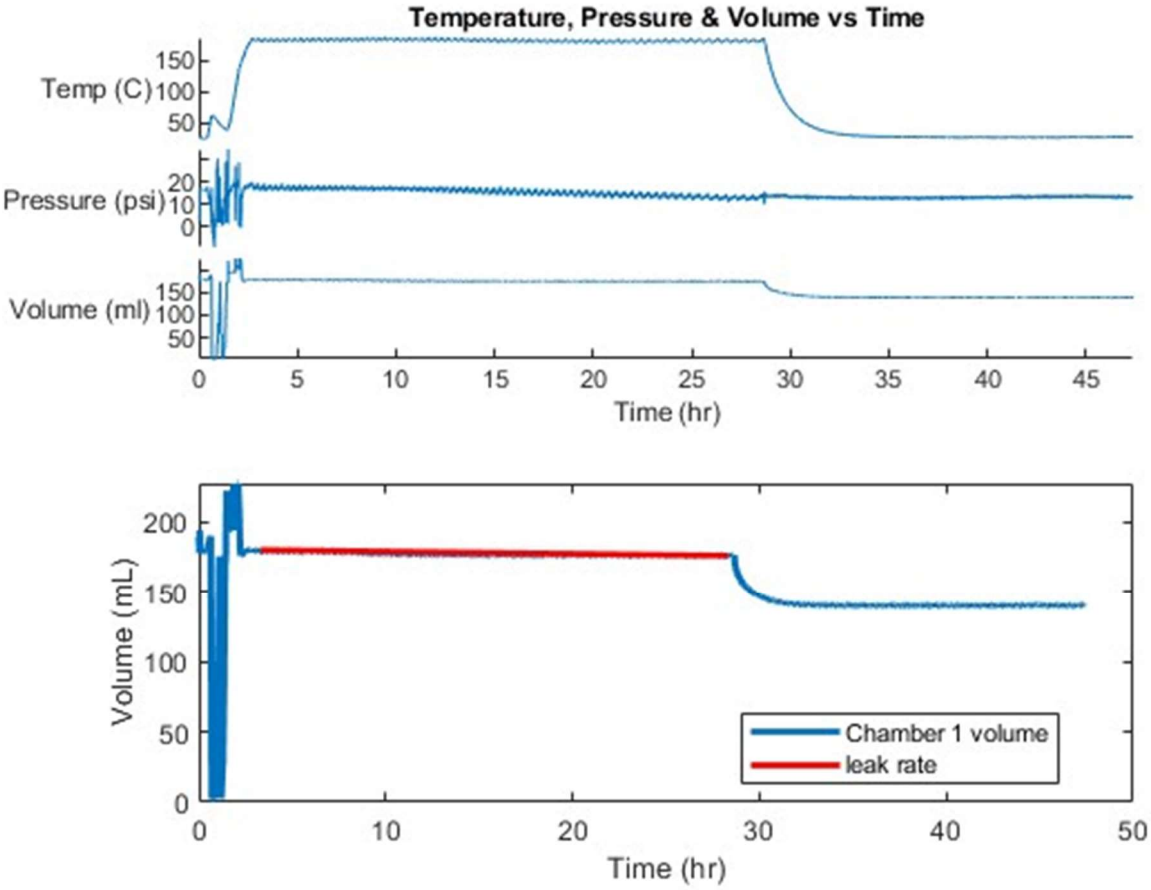


Figure 24: 25 hours leak rate at 10,000 RPM

The drastic decrease in the leak rate is a sign of seal performance improvement. This is proof that the leak rate reduces to stable value as the length of the experiment increases for a seal tested within manufacturer RPM range.

4.3 Testing seal beyond RPM range

This section evaluates the leak rate and discusses the results for a seal tested beyond the recommended manufacturer's RPM range. The seal is evaluated by analyzing the volume leak rate through the seal from the primary chamber to the secondary and tertiary chambers at an increasing rate of RPM past the manufacturer recommendation. The seal is tested at an

increasing RPM speed with testing temperatures of 180°C ± 3°C and pressure of 15 psi ± 3 psi in the in the primary chamber. The manufacturer's seal RPM limit is set for 7000 RPM. The seal is tested at 6500 RPM, below the manufacturer's RPM limit, and then at 7500 RPM, 8500 RPM and 9000 RPM.

4.3.1 6500 RPM

Figure 25 shows seal test at 6500 RPM for a 50-hour. Chamber 1 experiences a total volume loss of 1.33mL over a span of 48.45 hours bringing the leak rate to be 1.23 mL/hr.

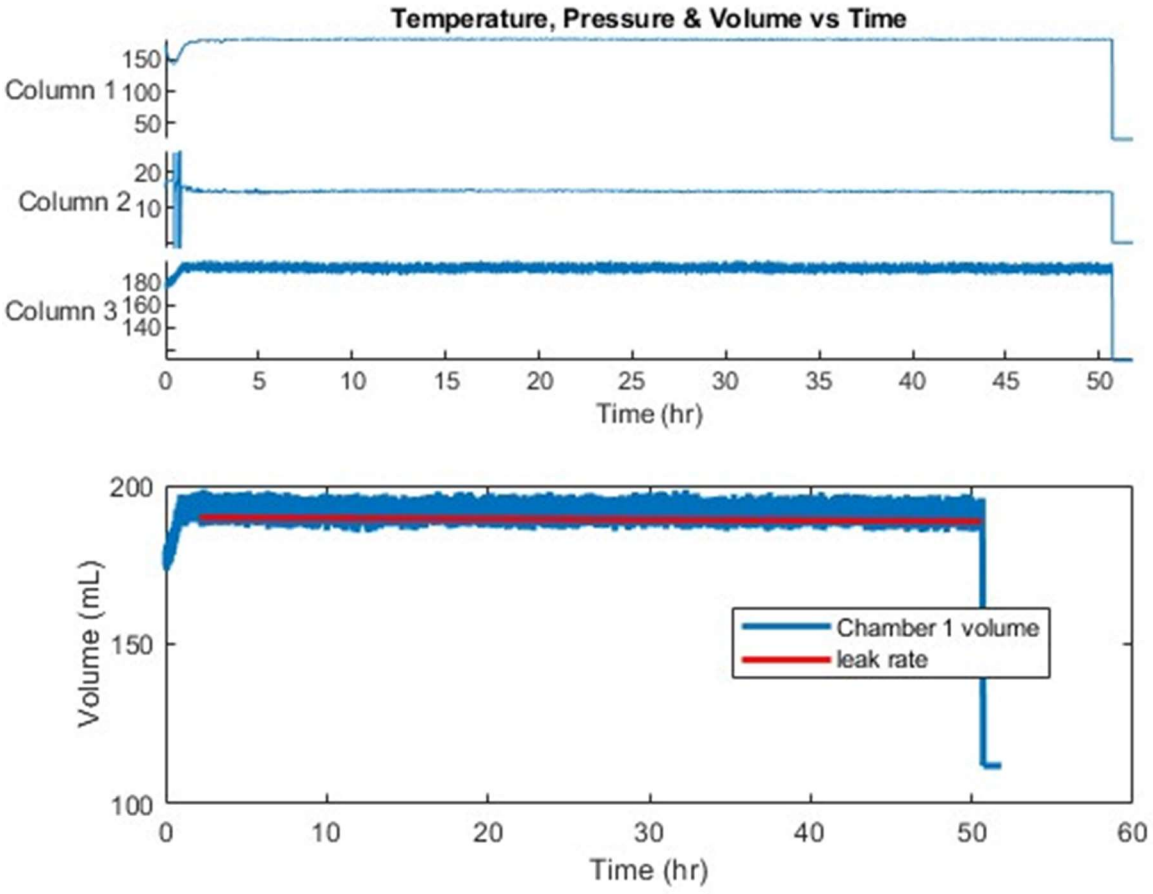


Figure 25: 50 hours leak rate at 6500 RPM

4.3.2 7500 RPM

Figure 26 shows seal test at 7500 RPM for a 68-hour. Chamber 1 experiences a total volume loss of 5.32mL over a span of 68.645 hours bringing the leak rate to 0.077 mL/hr.

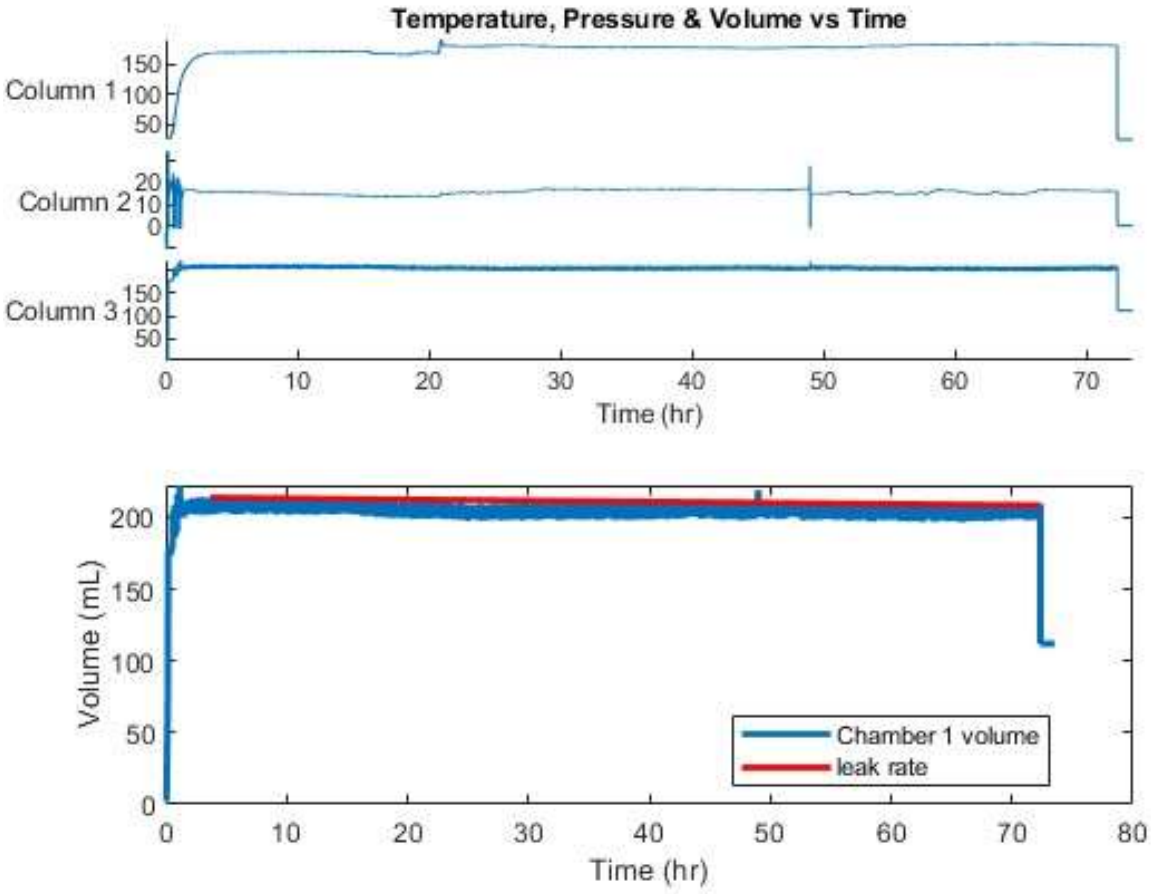


Figure 26: 70 hours leak rate at 7500 RPM

4.3.3 8500 RPM

Figure 27 shows seal test at 8500 RPM for a 48-hour. This test is a continuation of the of the test at 7500 RPM. Figure 27 indicates the point of increase of the RPM speed, the data thus experience a new stabilization period. The leak rate is evaluated over two different periods respectively highlighted in red and green in figure 27. The first one is evaluated right after the

RPM increase, and the second one starts after readjusted the pressure to the desired value of 15 psi after the previous pressure exceeded 18 psi. Both data are collected at the same RPM speed of 8500, they are consistent and demonstrate expected results. Chamber 1 experiences a total volume loss of 0.68mL over a span of 48.45. The leak rate before and after pressure adjustment are respectively calculated to be 0.02mL/hr and 0.01mL/hr.

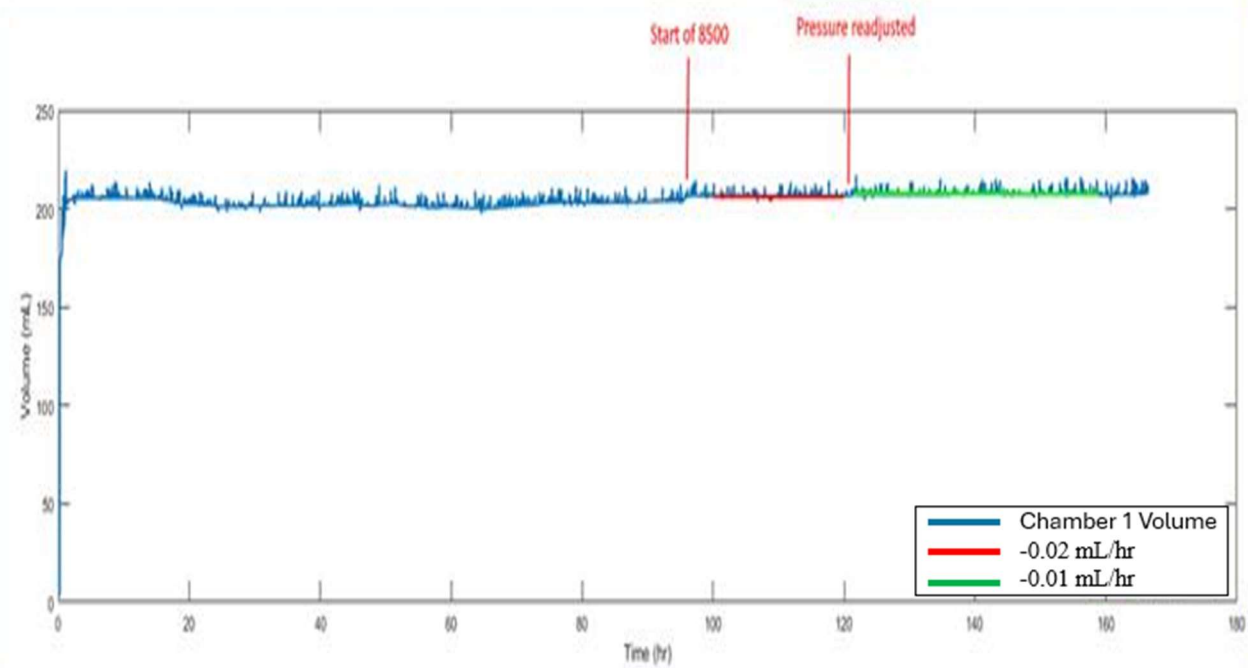


Figure 27: 48 hours leak rate at 8500 RPM

Figure 27 verifies the observed result established in section 4.2, leak rate of individual seals, that the leak rate reduces to stable value as the length of the experiment increases.

Furthermore, a synthesis of Figures 25, 26, and 27 demonstrates that the leak rate of a given seal reduces as the RPM speed increases.

4.3.4 9000 RPM

The seal is tested at 9000 RPM and the leak rate is evaluated at 24 hours increment. The RPM speed is already well beyond the recommended manufacturer limit of 7000 RPM, but an analysis of the leak rate may reveal the behavior of a seal when experiencing a failure.

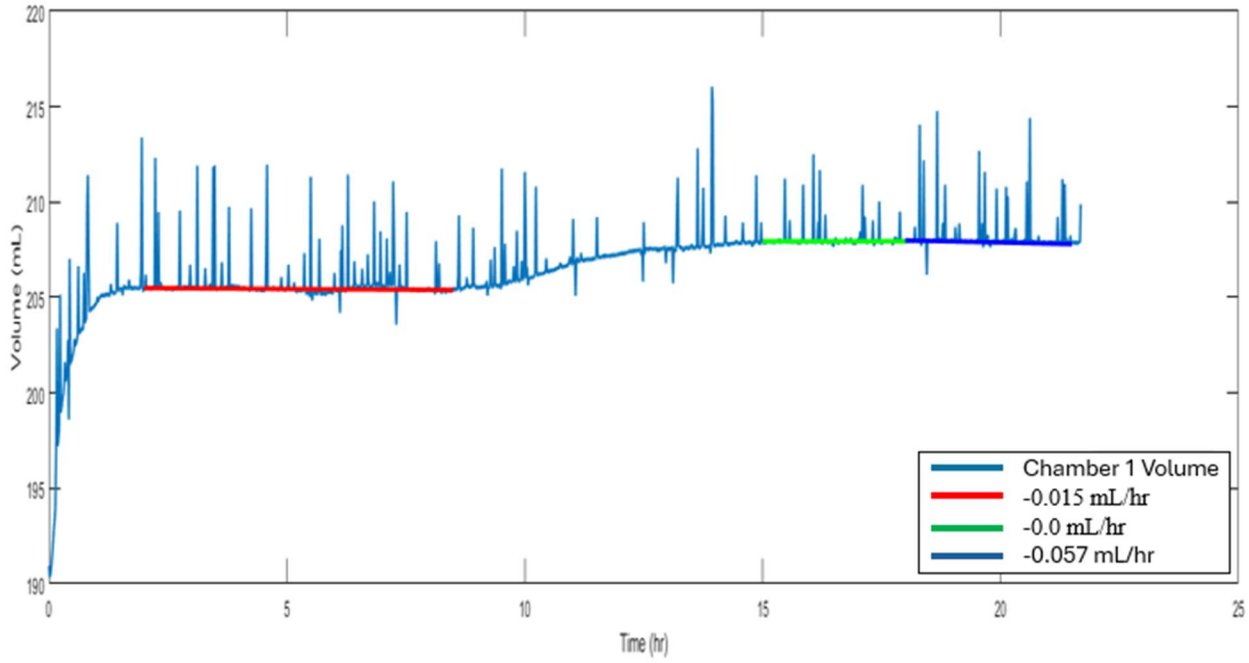


Figure 28: 24 hours leak rate at 9000 RPM

Figure 28 shows seal test at 9000 RPM for the first 24 hours. Chamber 1 experiences two separate zones of leak rates respectively highlighted in red, green and blue in figure 28. The first one is estimated to be 0.015mL/hr. After an unstable period, likely due to temperature control from the PID to maintain the temperature at 180°C $\pm$ 3°C, The leak rate zone highlighted in green experiences close to no volume loss, the leak rate is disregarded. The third leak rate is estimated to be 0.057 mL/hr. This leak rate is higher than the previous one, contrasting the results established above.

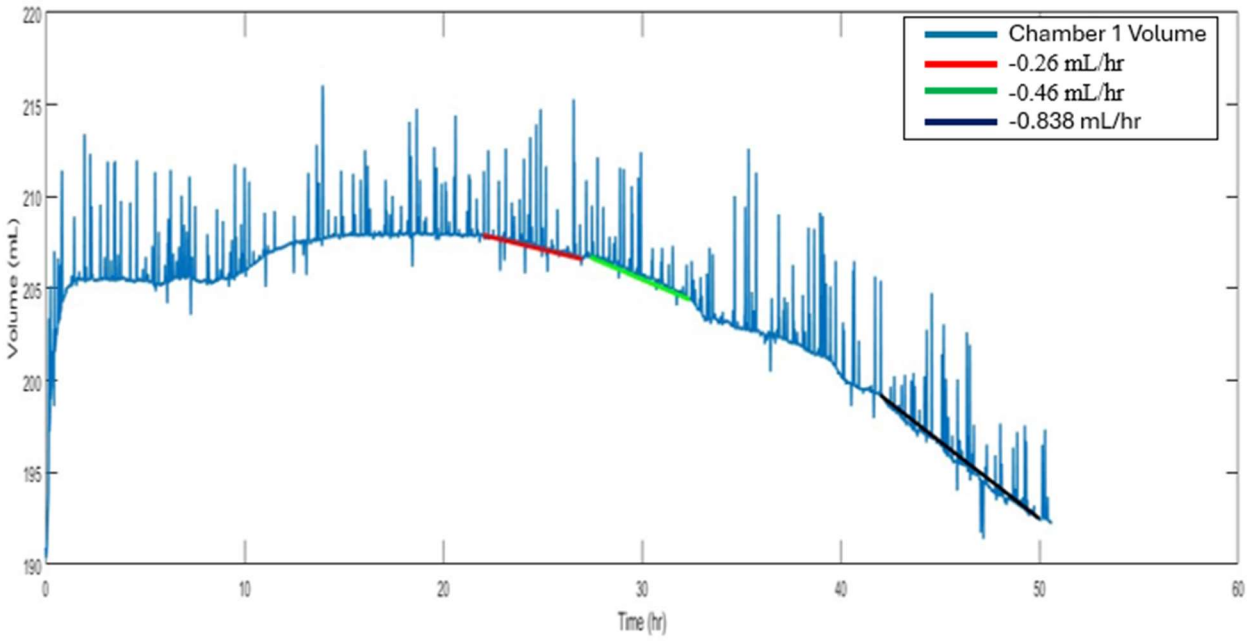


Figure 29: 48 hours leak rate at 9000 RPM

Figure 29 shows leak rate results at 9000 RPM for 48 hours. The analysis of Figure 29 is centered from 24-48 hours as the first 24 hours have already been studied above. Chamber 1 experiences three designated zones of leak rates respectively highlighted in red, green and black in figure 31. The first one is estimated to be 0.26mL/hr. The second leak rate zone is estimated to be 0.46 mL/hr. The third leak rate zone is calculated to be 0.838 mL/hr. Chamber 1 volume starts rapidly dropping thus increasing the leak rate significantly. This unexpected leak rate increase indicates a potential failure of the seal.

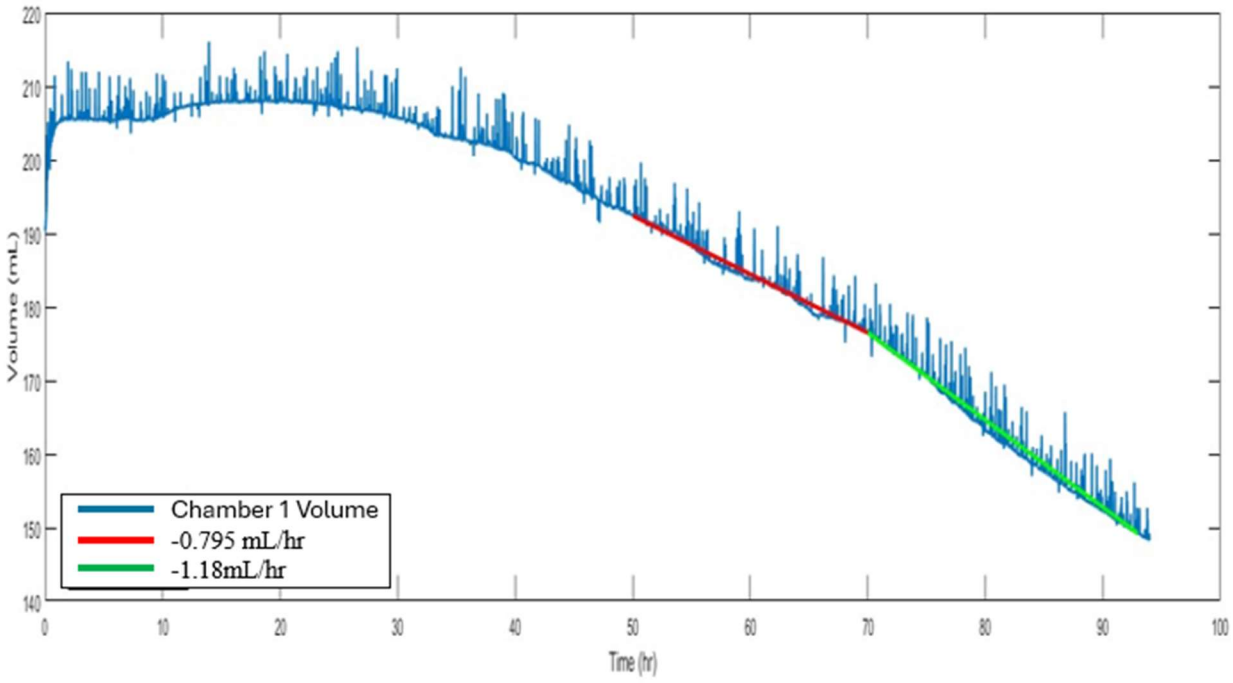


Figure 30: 96 hours leak rate at 9000 RPM

Figure 30 shows leak rate results at 9000 RPM for 96 hours. The analysis of Figure 30 is centered from 48 to 96 hours as the previous data have already been studied above. Chamber 1 experienced a leak rate of 0.795 mL/hr during the third 24-hour period, as highlighted in red in Figure 32. The leak rate over the fourth 24-hour period is estimated to be 1.18mL/hr from the 72 to 96-hour mark as highlighted in green in Figure 30. The trend of Figure 30 further reaffirms a likely seal failure.

4.4 Failures Analysis

This section asses the two failure mechanisms responsible for termination of an ongoing test. The two failure mechanisms experienced are seal failure and system malfunction failure.

4.4.1 Seal failure

Seal failure during the 10K RPM experiment typically arises from physical damage or weakening of the seal caused by test conditions surpassing its capacity. For example, in Figures 28, 29, and 30, the seal is subjected to testing at 9000 RPM, with the assessment of leak rate persisting until seal failure ensues. Despite surpassing the manufacturer's advised limit of 7000 RPM, analyzing the leak rate offers valuable understanding of the seal's behavior under failure circumstances. Figures 31 present the leak rate behavior for a seal tested beyond its limits.

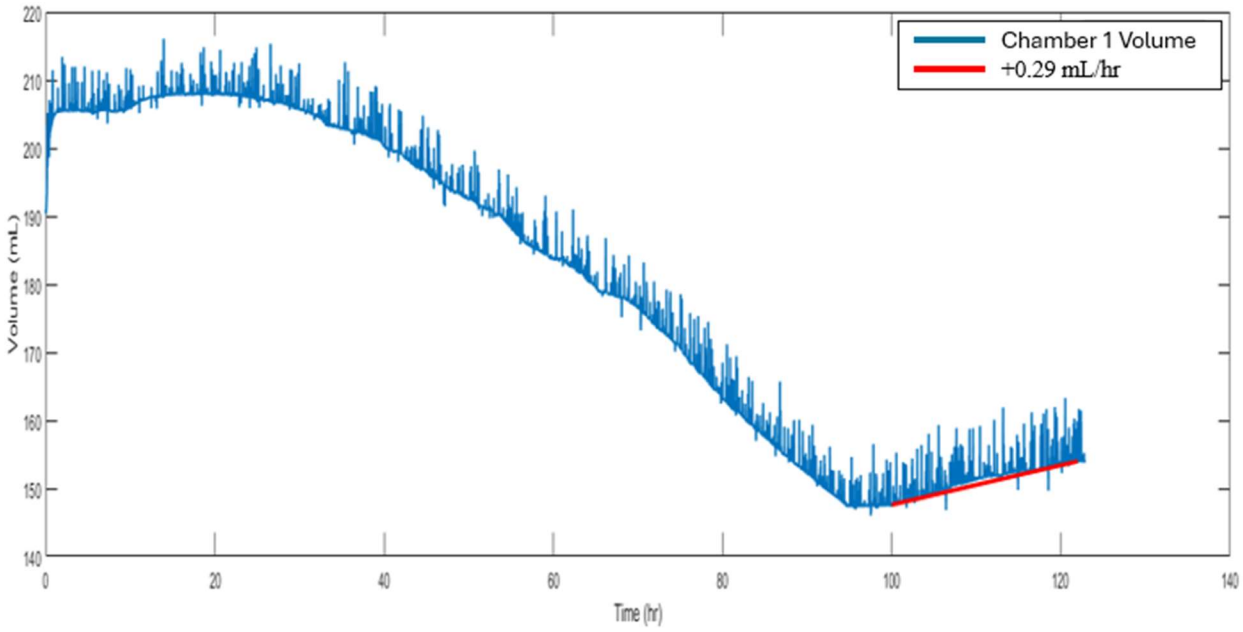


Figure 31: 120 hours leak rate at 9000 RPM

Figure 31 shows leak rate results at 9000 RPM for 120 hours. The analysis of Figure 31 is centered from 100 hours as the previous data have already been studied above. Chamber 1 experiences a gain in volume at a rate of 0.29 mL/hr from the 100 hours mark as highlighted in red in Figure 31. In Figure 31, the data presents a relatively steady leak rate in the first 24 hours period before rapidly losing volume over shorter periods of time until the primary chamber starts gaining fluid. Such phenomenon, for the purpose of this thesis only, will be denominated reverse

leak rate. The reverse leak rate occurs when the primary chamber starts gaining fluid instead of losing it. This positive gain in volume is definitive proof that the seal is damaged beyond repair as the only way volume would increase in the primary chamber is if it is coming from the secondary chamber thus confirming a seal failure. The analysis of the leak rate beyond its manufacturer speed limit demonstrates the behavior of a seal when experiencing failure.

4.4.2 System malfunction failure

A system malfunction failure is an abrupt test ending resulting from a mechanical issue.

6.4.2.1 Spring collar failure

Spring collar failure occurs when the coupler connecting the DUT shaft to the motor breaks. This results in the motor spinning continuously without rotating the shaft anymore. Figure 32 illustrates one of the fractured spring collars observed during a seal test within manufacturer speed limit at 10,000 RPM.



Figure 32: Shattered spring collar

Upon inspection of the spring collar, it became evident that the failure occurred due to shear forces, signifying that the torque needed to turn the DUT shaft surpassed typical levels, leading to stress beyond the material's capacity. Furthermore, scratches were detected where the DUT shaft was fastened to the spring collar, indicating wear that caused the black coating to be rubbed off, exposing a silver hue underneath, suggesting shaft slippage on the spring collar. A shattered spring collar is not apparent to naked eye alone but also on a leak rate study of the seal.

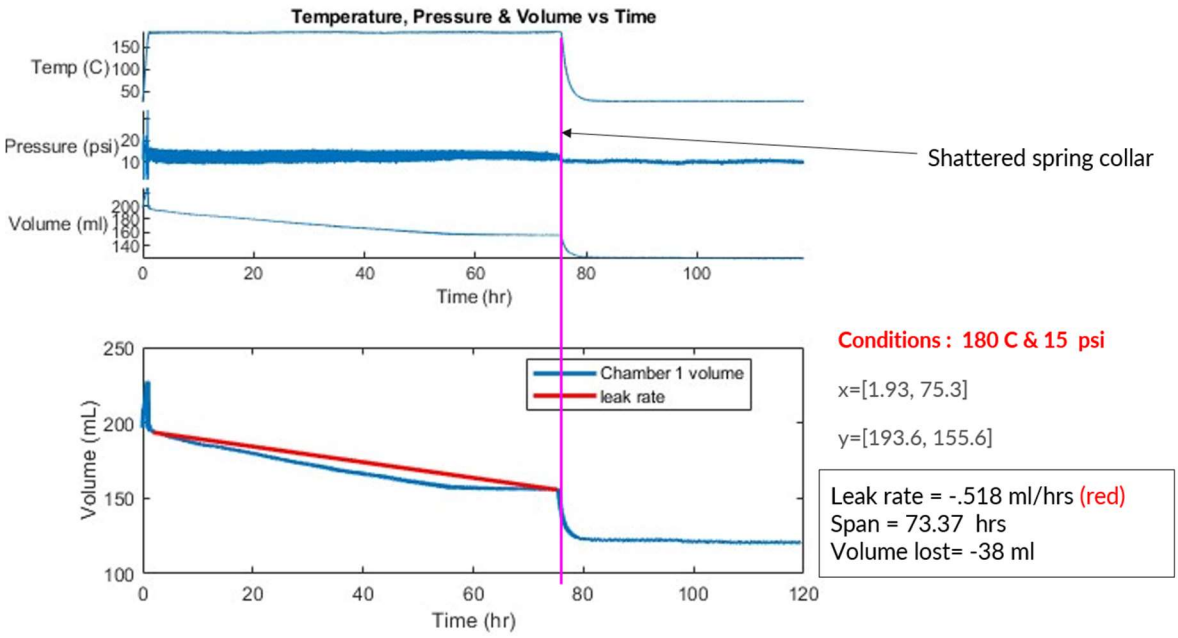


Figure 33: Leak rate behavior of test experiencing shattered collar

Figure 33 illustrates the leak rate behavior of test experiencing shattered collar. The graph shows the exact location of the shattered collar relative to the x-axis. The breaking point occurs at about the 75 hours mark as seen in Figure 33. The analysis of the volume leak rate alone can identify a shattered spring collar in a seal test experiment. The experiment in this figure is set at 10,000 RPM. Inside the primary chamber, the oil volume expands due to the increased temperature associated with high-speed rotation, then starts leaking a small, significantly reduced amount of volume over time, which helps determine the leak rate. When a spring collar shatters, the motor keeps spinning while the DUT shaft does not. The temperature and expanded volume evidently shrink back to room temperature values at the same rate as can be seen past the pink vertical line in Figure 33.

Chapter 5: Conclusion and Future Work

5.1 Conclusion

Mechanical sealing technology is widely used where high-speed sealing is required – including the oil and gas industry. Even with modern-day engineering simulation software that can help with understanding critical aspects of mechanical seal design, an experimental evaluation of these seals is still an important aspect of characterization. This thesis addresses the performance of the mechanical seal through the evaluation of the leak rate. It also provides an insight into the test equipment, data acquisition system used and testing conditions of the experiment. The leak rate analysis performed provides the following conclusions to the research objectives established in Chapter 1:

Objective 1. Explore the impact of mechanical seal usage on leak rate efficiency.

The impact of mechanical seal usage on leak rate efficiency is studied in section 4.2. A correlation is found between the efficiency of the leak rate and the duration of the experiment, when the experiment is within the manufacturer specified speed only. Indeed, the leak rate efficiency increases, or the leak rate reduces, to stable value as the length of the experiment increases for a seal tested within manufacturer's RPM range. On the other hand, prolonged testing experiments beyond the recommended rotary speed provided by manufacturer lead to a rapid volume loss thus a decrease in leak rate efficiency.

Objective 2. Investigate the relationship between rotary speed and mechanical seal leak rates.

The study investigated the leak rate of a specific mechanical seal as the rotary speed increased gradually, starting from speeds below the manufacturer's recommended limit and progressing until reaching a predetermined threshold. This study namely tested the mechanical seal at the speed range of 6500 RPM, 7500 RPM and 8500 RPM for a manufacturing speed limit estimated at 7000 RPM. Each test lasted at least 48 hours and the results of all three leak rate values are respectively, from lowest speed to highest, 1.23 mL/hr, 0.077 mL/hr, and 0.01mL/hr. Thus showing that the leak rate of a given mechanical seal reduces, or the leak rate efficiency increases, as the RPM speed increases only up to a certain rotary speed beyond the manufacturer's range.

Objective 3. Subject mechanical seals to non-standardized conditions to induce seal failure.

The ultimate goal of this objective was to analyze the leak rate behavior of mechanical seal experiencing failure. But in order to do so, one must first induce a mechanical seal failure, if at all possible. The study explored that a mechanical seal failure could be provoked by putting the seal under harsh, yet controlled, testing conditions. The three conditions controlled in this study are the temperature, pressure, and rotary speed of the seal. The variables are selected for its control effect, operational safety, and efficiency. It became apparent that increasing the rotary speed of the seal beyond manufacturer’s recommended range was the most efficient and most importantly safest approach of inducing failure in the seal. The tested mechanical seal with 7000

RPM manufacturing speed limit set by the manufacturer shows ultimately fails at 9000 RPM. Mechanical seal failure can thus be induced with an increase RPM speed beyond the manufacturer's RPM range.

Objective 4. Analyze the leak rate behavior of mechanical seal experiencing failure.

This objective was to evaluate the leak rate behavior of a mechanical seal experiencing failure. An in-depth analysis of sections 4.3.4 and 4.4.1 provided insight on the leak rate behavior of mechanical seals experiencing failure. The seal failure in this experiment was noticed at the speed of 9000 RPM for a seal speed limit recommendation at 7000 RPM. Seal failure became noticeable approximately 20 hours into the experiment, marked by a gradual decline in leak rate efficiency over time, contradicting the initial objectives. Subsequently, there was a sharp increase in fluid loss within brief intervals, resulting in a considerably higher calculated leak rate, indicating a deterioration in the mechanical seal's performance. The fluctuating leak rate signifies the seal's failure to sustain a consistent performance as the experiment progresses. Nonetheless, the breaking point is shown when the primary chamber starts gaining fluid. The reverse leak rate is proof that the mechanical seal has failed beyond repair. Hence, under extreme rotary speed conditions beyond the recommended limit, the leak rate experiences seals failure by drastically losing volume within shorts periods of time. If prolonged experiment continues, the mechanical seal will be damaged beyond repair and the leak rate will present a reverse leak rate where the primary chamber is gaining volume instead of losing it.

5.2 Future Work

Although this thesis has undertaken extensive research, there is still room for improvement. The following recommendations outline areas for further investigation into the performance tests and evaluation of mechanical seals.

The first recommendation would be to broaden the assessment of the seal's performance beyond just leak rate, incorporating criteria like its resilience to extreme conditions. Secondly, after analyzing the leak rate patterns of failed mechanical seals, the next phase should involve examining the microscopic impact of such failures. These investigations are vital for averting damage to mechanical seals, which can lead to significant delays and expenses in large-scale oil and gas projects because sealing technologies are expensive, and repairs are just as costly and time consuming. Thirdly, this research currently focuses solely on induced mechanical failures due to extreme rotary speeds while holding temperature and pressure constant. How would the leak rate behave when the condition beyond standard range is the temperature or pressure? Would it have the same impact on the leak rate? The same damage on the mechanical seal? It is crucial to explore how variations in temperature or pressure outside standard ranges affect leak rates and seal damage. One way to approach this study would be to have a structured three-step methodology, where each phase isolates one variable condition while keeping the others constant, thus studying the seal's leak rate until failure occurs. While this thesis provides a solid foundation by establishing results for rotary speed variations with constant temperature and pressure, it's constrained by significant limitations, notably in terms of time and finances.

References

[1] W. Lou, W. Zhang, X. Liu, W. Dai and D. and Xu, "Degradation of hydrogenated nitrile rubber (HNBR) O-rings exposed to simulated servo system Conditions," *Polymer Degradation and Stability,* vol. 144, pp. 464-472, 2017.

[2] X. Liu, W. Zhang, W. Lou and Y. X. a. D. W. Huang, "Investigation on thermal oxidative aging of nitrile rubber (NBR) O-rings under compression stress," *IOP Conference Series: Materials Science and Engineering,* vol. 265, no. 1, p. 012003, 2017.

[3] R. Pazur, J. Cormier and K. and Korhan-Taymaz, "Service life determination ofnitrile O-rings in hydraulic fluid," *Rubber Chemistry and Technology,* vol. 87, no. 2, pp. 239-249, 2014.

[4] A. Mosallam, K. Medjaher and N. and Zerhouni, "Data-driven prognostic method based on Bayesian approaches for direct remaining useful life prediction," *Journal of Intelligent Manufacturing,* vol. 27, no. 5, pp. 1037-1048, 2016.

[5] F. Guo, X. Jia, M. Lv, L. Wang, R. F. Salant and Y. and Wang, "The effect of aging in oil on the performance of a radial lip seal," *Tribology International,* vol. 78, pp. 187-194, 2014.

[6] F. Guo, X. Jia, L. Huang, R. F. Salant and Y. and Wang, "The effect of aging during storage on the performance of a radial lip seal," *Polymer degradation and stability,* vol. 98, no. 11, pp. 2193-2200, 2013.

[7] A. Sharma, M. Amarnath and P. and Kankar, "Feature extraction and fault severity classification in ball bearings," *Journal of Vibration and Control,* vol. 22, no. 1, pp. 176-192, 2016.

[8] S. Dong and T. and Luo, "Bearing degradation process prediction based on the PCA and optimized LS-SVM model," *Measurement,* vol. 46, no. 9, pp. 3143-3152, 2013.

[9] J. Yu, "Bearing performance degradation assessment using locality preserving projections," *Expert Systems with Applications,* vol. 38, no. 6, pp. 7440-7450, 2011.

[10] M. Ramachandran, *Intelligent Condition Monitoring and Prognostic Methods with Applications to Dynamic Seals in the Oil & Gas Industry,* Norman: Ph.D dissertation, Gallogly College of Engineering, Oklahoma University, 2019.

[11] R. Flitney, Seals and sealing handbook, Sixth edition ed., Amsterdam: Butterworth-Heinemann, an imprint of Elsevier: ed. iChemE, 2014, p. 633.

[12] R. Perry, *A Modular Approach To The Development Of A Product Platform For Mechanical Seal Characterization,* Norman: M.S dissertation, Gallogly College of Engineering, Oklahoma University, 2020.

[13] A. Bicak, "OU 10K-RPM Documentation & Testing Procedure," Gallogly College of Engineering, Oklahoma University, Norman, 2022.

[14] N. Khor, "10K Operating Manual," Gallogly College of Engineering, Oklahoma University, Norman, 2023.

Appendix A: Nomenclature and Acronyms

10K or 10K RPM:	Testing System at 10,000 rpm
Chamber 1:	Primary Chamber
DAQ:	Data Acquisition System
DUT:	Device Under Testing
EHL:	Elastohydrodynamic
hr:	Hours
LVDT:	Linear Variable Differential Transformer
mL	Milliliters
PID	Proportional-Integral-Derivative
PTFE:	Polytetrafluoroethylene
PSI1:	Primary Chamber Pressure
RPM:	Rotary speed
TC6:	Primary Chamber Temperature
.TXT:	Tab-delimited
VOL1:	Primary Chamber Volume